SANDIA REPORT
SAND2019-10184
Printed Click to enter a date

Sandia National Laboratories

Applying Waveform Correlation to Aftershock Sequences Using a Global Sparse Network

Amy Sundermier
Rigobert Tibi
Christopher J. Young

Prepared by
Sandia National Laboratories
Albuquerque, New Mexico
87185 and Livermore,
California 94550

Issued by Sandia National Laboratories, operated for the United States Department of Energy by National Technology & Engineering Solutions of Sandia, LLC.

NOTICE: This report was prepared as an account of work sponsored by an agency of the United States Government. Neither the United States Government, nor any agency thereof, nor any of their employees, nor any of their contractors, subcontractors, or their employees, make any warranty, express or implied, or assume any legal liability or responsibility for the accuracy, completeness, or usefulness of any information, apparatus, product, or process disclosed, or represent that its use would not infringe privately owned rights. Reference herein to any specific commercial product, process, or service by trade name, trademark, manufacturer, or otherwise, does not necessarily constitute or imply its endorsement, recommendation, or favoring by the United States Government, any agency thereof, or any of their contractors or subcontractors. The views and opinions expressed herein do not necessarily state or reflect those of the United States Government, any agency thereof, or any of their contractors.

Printed in the United States of America. This report has been reproduced directly from the best available copy.

Available to DOE and DOE contractors from
U.S. Department of Energy
Office of Scientific and Technical Information
P.O. Box 62
Oak Ridge, TN 37831

Telephone: (865) 576-8401
Facsimile: (865) 576-5728
E-Mail: reports@osti.gov
Online ordering: http://www.osti.gov/scitech

Available to the public from
U.S. Department of Commerce
National Technical Information Service
5301 Shawnee Rd
Alexandria, VA 22312

Telephone: (800) 553-6847
Facsimile: (703) 605-6900
E-Mail: orders@ntis.gov
Online order: https://classic.ntis.gov/help/order-methods/

ABSTRACT

Agencies that monitor for underground nuclear tests are interested in techniques that automatically characterize earthquake aftershock sequences to reduce the human analyst effort required to produce high-quality event bulletins. Waveform correlation is effective in detecting similar seismic waveforms from repeating earthquakes, including aftershock sequences. We report the results of an experiment that uses waveform templates recorded by multiple stations of the Comprehensive Nuclear-Test-Ban Treaty International Monitoring System during the first twelve hours after a mainshock to detect and identify aftershocks that occur during the subsequent week. We discuss approaches for station and template selection, threshold setting, and event detection that are specialized for aftershock processing for a sparse, global network. We apply the approaches to three aftershock sequences to evaluate the potential for establishing a set of standards for aftershock waveform correlation processing that can be effective for operational monitoring systems with a sparse network. We compare candidate events detected with our processing methods to the Reviewed Event Bulletin of the International Data Center to develop an intuition about potential reduction in analyst workload.

ACKNOWLEDGEMENTS

This research was initiated by members of the Comprehensive Nuclear-Test-Ban Treaty Organization (CTBTO) and experts that attended the October 2018 CTBTO Expert Meeting on Advances in Waveform Processing and Special Studies in Vienna, Austria. The following people attended the initial project launch meeting to set the guidelines and parameters for using methods of waveform correlation to detect aftershock events for four earthquakes, and are acknowledged as contributors to the experimental design:

Helmuth Breitenfellner, Steven J. Gibbons, Ivan Kitov, Tormod Kvaerna, Ronan Le Bras, Christos Saragiotis, Megan Slinkard, and Amy Sundermier.

Ronald A. Brogan reviewed SeisCorr template libraries and correlation jobs and provided advice on filter bands for signal enhancement.

CONTENTS

LIST OF FIGURES

LIST OF TABLES

This page left blank

ACRONYMS AND DEFINITIONS

Abbreviation	Definition
CSS	Center for Seismic Studies
CTBT	Comprehensive Nuclear-Test-Ban Treaty
CTBTO	Comprehensive Nuclear-Test-Ban Treaty Organization
IDC	International Data Centre
IMS	International Monitoring System
LTA	Long-Term Average
NDEF	In the CSS standard, this is defined as the number of locating phases. We use this term here to mean the number of detecting templates in a multistation validation job.
REB	Reviewed Event Bulletin
SEL	Standard Event List
SNL	Sandia National Laboratories
SNR	Signal-to-Noise Ratio
STA	Short-Term Average
STA/LTA	Ratio of Short-Term Average over Long-Term Average

1. INTRODUCTION

Several studies have shown that waveform correlation is effective in detecting similar seismic waveforms from repeating earthquakes, including aftershock sequences. Aftershock sequences from large earthquakes greatly increase the number of seismic events that are detected on global networks such as the International Monitoring System (IMS), which results in increased analyst workload and may lead to delays in bulletin publication. For that reason, monitoring agencies have shown interest in adopting techniques such as waveform correlation to quickly characterize aftershock sequences and hence reduce the amount of effort required by analysts to produce a high-quality event bulletin during an aftershock sequence. Members of the Comprehensive Nuclear-Test-Ban Treaty Organization (CTBTO) invited several experts familiar with waveform correlation methods to participate in a study of four aftershock sequences that were particularly problematic for the International Data Centre (IDC). The goal of the study was to reduce analyst workload in monitoring system pipelines during time periods of high event rates associated with aftershock sequences. The study was conducted in parallel by different researchers using the same four aftershock sequences; the CTBTO plans to evaluate the results as part of a prototype pipeline.

This report describes the research conducted at Sandia National Laboratories (SNL) on the aftershock sequences identified by the CTBTO members. The authors used SeisCorr, a software system developed at SNL for waveform correlation event detection that has previously been used for studies of aftershock sequences [1][2] and general regional seismicity [3]. Our experiment uses multiple IMS station waveform templates from events automatically detected and located by IDC data processing during the first 12 hours after the mainshock, to detect and identify aftershocks that occur during the subsequent week. Using the SeisCorr system, methods were developed for station and template selection, threshold setting, and event detection that are specialized for aftershock processing using sparse, global networks. The specialized methods were applied to three of the four aftershock sequences to evaluate the potential for establishing a set of standards for aftershock waveform correlation processing that can be effective for operational monitoring systems that use a sparse network such as the IMS. To evaluate the effectiveness of the methods, the bulletin of candidate events detected with our specialized aftershock processing methods are compared to the Reviewed Event Bulletin (REB) to develop an intuition about potential reduction in analyst workload.

2. EXPERIMENT METHODS AND RESULTS

The research described in this report applies waveform correlation technique to three aftershock sequences, and will hereafter be referred to as the aftershock study. The basic experimental design was created by consensus at an international meeting, but the application of SNL's SeisCorr tool required some additional design decisions and technical refinements that are described in detail in this report.

Section 2.1 describes the four aftershock sequences chosen by the CTBTO for the study and general guidelines that were given to the researchers at the international meeting and project launch at the CTBTO in Vienna on October 11, 2018. Section 2.2 briefly describes SNL's application for seismic waveform correlation, including the features of the SeisCorr software. Sections 2.3 through 2.5 provide details about the aftershock study and readers that are familiar with waveform correlation and the aftershock study may choose to begin reading with those sections. Section 2.3 describes the selection of stations, waveform templates, and template threshold setting processes to prepare for waveform correlation of each aftershock sequence. Section 2.4 provides an overview of the correlation processing for the aftershock study. Section 2.5 Multistation Validation provides an overview on how SeisCorr organizes correlation detections into candidate events and describes in detail the method to choose tolerances for grouping the detections and the study results.

2.1. Experimental Setup

The CTBTO chose four aftershock sequences for study that had proven particularly problematic for the IDC because the event rate during each of these sequences was much higher than normal, leading to extremely high analyst workload to produce the REB. The CTBTO set the geographical footprint and temporal span for each aftershock sequence for the study, and provided guidance to use historical waveform templates and/or waveform templates from the automatic Standard Event List 3 (SEL3) to detect events that occurred later in time; in other words, to provide results useful for an operational system, template waveforms must chronologically precede the waveforms that are processed for detections. The research described in this report was based on the discussions that occurred in Vienna in October 2018 during a side meeting to the CTBTO Expert Meeting on Advances in Waveform Processing and Special Studies, which hereafter will be referred to as the project launch meeting. Additional information was provided to study participants through a collaboration website that is access controlled and maintained by the CTBTO. The maps and geographical footprints of the aftershock sequences were obtained from this collaboration website and are included in this report for the convenience of the reader.

The research described in this report was proposed and funded before the CTBTO had finalized all the details of the study on the collaboration website. Thus, the research is largely based on discussions during the project launch meeting in Vienna and was limited by the funds acquired based on a proposal written with information from the launch meeting.

NOTE: To aid in proposing follow-up research, the report includes notes such as this one with descriptions of additional work if more funding becomes available, as well as issues that were discovered during the study.

The four aftershock sequences identified by the CTBTO are listed in Table 2-1. The geographical footprint of the aftershock sequences specifies the location of events that may be used to create historical waveform templates and bounds the area for comparing detected events with REB events. The geographical footprints for the 2015 Nepal and 2018 Papua New Guinea sequences are given as a 3-degree radius from the location identified by latitude and longitude. The geographical footprints for the 2015 Chile and 2011 Tohoku sequences are given as a box bounded by latitude/longitude minimum and maximum values. The temporal span specifies the time window of the dataset for the study, which is the same for all four aftershock sequences. The temporal span is $[t_0, t_0 + 7 \text{ days}]$, where t_0 is the mainshock origin time.

Table 2-1. Aftershock sequences identified by CTBTO.

Sequence	Mainshock Origin Time (UTC)	Mainshock Magnitude (M_w)	Geographical Footprint
2015 Nepal	2015-APR-25 06:11:25	7.8	3° radius from [28.230°N, 84.731°E, 8.2 km depth]
2018 Papua New Guinea	2018-FEB-25 17:44:44	7.5	3° radius from [6.068°S, 142.768°E, 23.4 km depth]
2015 Chile	2015-SEP-16 22:54:32	8.3	box 28°--34°S, 71°--75°W
Tohoku, Japan 2011	2011-MAR-11 05:46:24	9.0	box 32°--44°N, 140°--146°E

The CTBTO provided maps with the event locations for the four aftershock sequences on the collaboration website, which are shown in Figure 2-1.

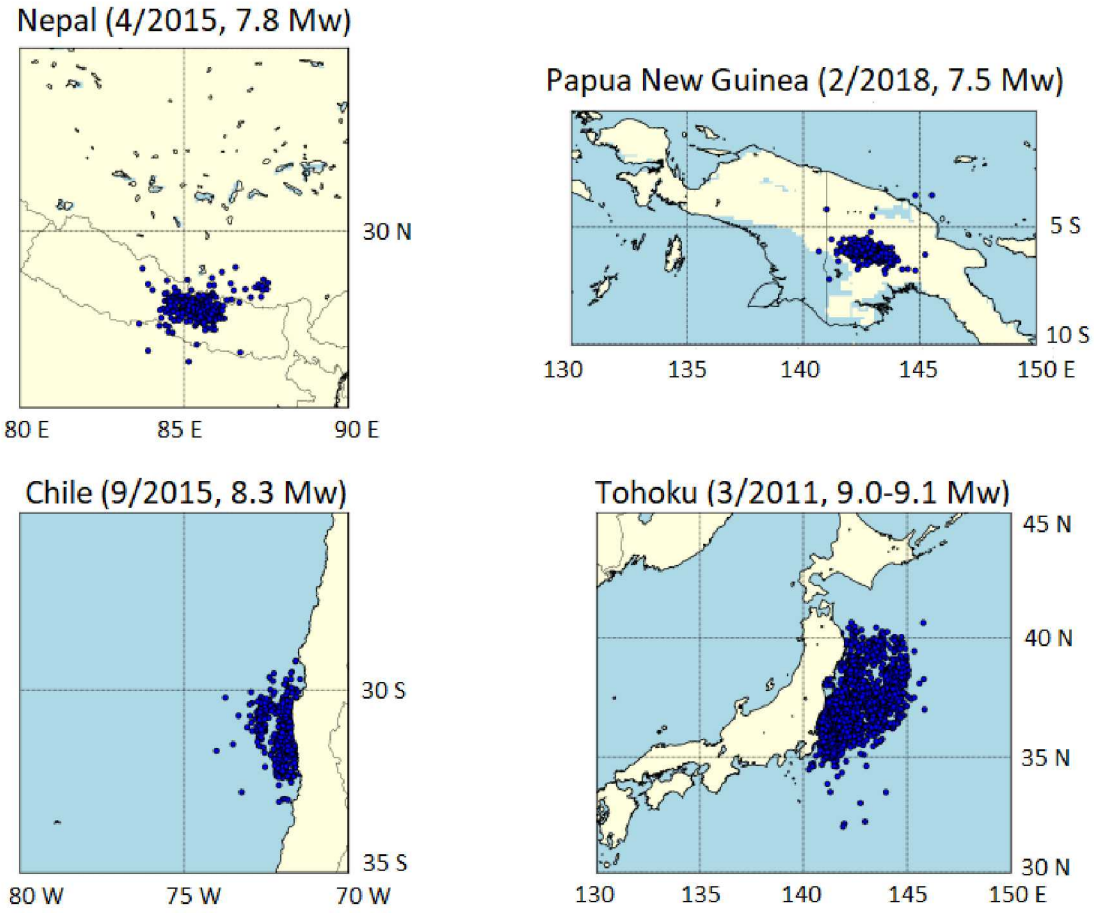

Figure 2-1. CTBTO maps of the four aftershock sequences. Blue dots represent aftershock locations.

In addition to aftershock events in the first 12 hours after the mainshock, the guidance provided by the CTBTO at the project launch meeting allowed template waveforms to be created from any events published in IDC bulletins that preceded the mainshock. The two options discussed below included the following potential sources of template waveforms:

- SEL3 – An automatic bulletin that is available within hours after the mainshock. The discussion at the project launch meeting stated that SEL3 is available within 12 hours. The automatic bulletin is not reviewed by analysts, thus the association of detections into events may be inaccurate and lead to poor event locations. The advantage to choosing SEL3 as the source of template waveforms is that SEL3 is available for any aftershock sequence because it is automatically created by the IDC pipeline. In other words, a large earthquake from a fault that has not been active during the recent decades of digitized waveforms would still have 12 hours of SEL3 waveform templates from aftershocks, even if there were no historical digital waveform records of that fault.
- REB – The analyst reviewed bulletin is available 3 days after the mainshock. The discussion at the project launch meeting suggested that historical REB events from the same region could be used as template waveforms. The advantage to using REB events is that the locations and associations are much more likely to be accurate. The disadvantage to using REB events is that much more effort is involved in choosing the template events to use for the aftershock study, since it is possible that the region of study encloses events from multiple source types (e.g., mining blasts) that are not desired as templates for the aftershock sequences. Unfortunately, there is no easy way to differentiate source types in the event bulletins when choosing events for earthquake templates.

The method chosen for this research uses only events from SEL3 to generate templates, i.e. we do not utilize templates from REB events that preceded the mainshock. This approach is visually described by the timeline shown in Figure 2-2. Templates are created from the automatic catalog events in the first 12 hours after the mainshock, then the templates are correlated against the next week of continuous data to detect subsequent aftershocks. Note that the SEL3 events we use may precede the mainshock, and where foreshocks were found, they were included as candidate templates.

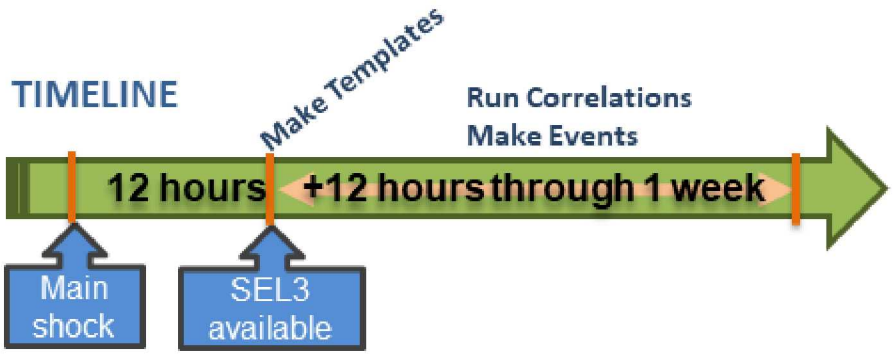

Figure 2-2. Timeline for template building and events detections.

The method was chosen to be compatible with existing operational pipelines. We desire to limit the number of additional steps that must be added to the operational pipeline, particularly any steps that require human intervention.

Further guidance was provided at the project launch meeting that the goal of the research is not to find more events than are listed in the REB, but rather to detect aftershocks included in the REB, which are currently built manually by IDC analysts. This is consistent with the main focus of this research project, which is to find out if waveform correlation can reduce the workload on analysts during large aftershock sequences by augmenting the events detected by the existing automatic IDC pipeline.

2.2. Overview of SeisCorr Software

The study was conducted using the SeisCorr software for waveform correlation, developed at SNL. It is important to recognize that SeisCorr has not been implemented for use in a real-time system. It was originally developed as a research tool to rapidly process of continuous waveform data recorded by a single station. An additional capability to screen out lower-quality events by performing multistation validation of individual station results was added later. While SeisCorr has an interactive user interface, it is meant to process large amounts of data without human review of the templates prior to their use in correlation jobs.

SeisCorr has been used for historical earthquake aftershock studies before, notably for the study of the Wenchuan aftershock sequence [1]. Those studies involved both IMS and local station networks. The current study is the first time that SeisCorr has been used to study an aftershock sequence using only IMS stations.

SeisCorr supports three major activities for waveform correlation research: 1) template preparation, 2) correlation of template waveforms with continuous waveform data to detect possible events, and 3) candidate event creation from multistation validation. The following subsections provide a high-level overview of these three SeisCorr activities, while specific methods and parameters chosen for the study for the stations, templates, and multistation validation are described later in the report.

SeisCorr uses the Center for Seismic Studies (CSS) version 3 database schema [4] for the Origin, Arrival, and Association tables. SeisCorr contains a specialized schema, not described in this report, of database tables for:

- waveform correlation
  - templates, and
  - template matches (i.e., detections), and
- multistation validation
  - candidate origins, and
  - candidate associations.

2.2.1. Template Preparation

SeisCorr contains functionality for the creation of a template library for a given station based on a query of the database arrival table. For the aftershocks study, arrivals were sought for events located within the geographic footprint of the sequence, which occurred within the time window from one week before the mainshock (i.e., foreshocks) to 12 hours after the mainshock. SeisCorr queries for labeled arrivals at the chosen station, and for the aftershock study, the phases Pg, Pn, and P from SEL3 were included in the arrival list. SeisCorr allows the user to filter the waveforms associated with each arrival using a bandpass filter chosen to work well for the epicentral distance of the

recording station. Then SeisCorr screens the filtered waveforms based on a specified STA/LTA threshold to eliminate waveforms with low signal-to-noise ratio (SNR), resulting in a set of candidate templates. The candidate templates can be saved as a template library for the station. We use the term "candidate template" to recognize that even after the SNR-screening step, not all arrival waveforms will make acceptable templates for correlation; additional screening steps may be applied to eliminate poor quality templates.

Metadata about the template waveforms are stored in a database table that contains columns such as ORID and ARID that allow the user to discover metadata about the template's corresponding event, such as location, magnitude, phase, and so on.

Prior waveform correlation research at SNL has demonstrated the importance of choosing a correlation coefficient threshold that is dependent on the characteristics of the template [3]. The distribution of correlation values obtained from correlating a template with a continuous data stream can be thought of as the sum of 2 distributions: 1) correlation of the template with noise, and 2) correlation with similar events. SeisCorr implements a sophisticated algorithm for setting template thresholds based upon a false alarm rate obtained from correlation with noise for each correlation threshold. Ordinarily, unless similar events can be identified and cut out first, correlating a template with continuous data will generate both noise and signal correlations. However, time-reversing the template ensures the template has the same time-bandwidth product as the template proper and should yield a very similar distribution of correlation values with noise windows, but also not correlate with similar events even if they are present. Thus, a time-reversed template can be correlated with continuous data without first screening out time windows with similar events to generate a robust distribution of noise correlation values. Using this algorithm, template thresholds can be set individually for each template, and the thresholds can be set for a consistent false alarm rate (FAR) based on noise correlations.

A recent study [5] has shown that for a template waveform with a low time-bandwidth product (e.g. teleseismic P) a threshold based solely on the noise distribution may be too low, because correlation with signals from some non-similar events do not fit within the noise distribution. Thus, for the aftershock study an adjustment was made to the time-reverse method to account for template waveforms based on teleseismic P and a global, sparse network. The template thresholds were set by the time-reverse method implemented in SeisCorr, but the duration of the aftershock sequence was processed to determine the noise correlation thresholds, i.e. we intentionally chose a time period with many events in it. Thus, the thresholds that were set for this study were based not only on correlation with noise but also with the numerous aftershocks. More research is needed to develop an optimal approach to setting thresholds for template waveforms for aftershock studies since the approach used in this study must be modified for an operational system; our approach violated the antecedent constraint by using waveform data throughout the duration of the aftershock sequence to set template thresholds to detect later events.

NOTE: Using the time-reverse threshold method for only the duration of the first 12 hours of the aftershock sequence would not violate real-time system constraints.

There are several steps required to create a template library in SeisCorr using an event bulletin as a source for template events. This section will describe the steps in general, and later sections will discuss the details for each aftershock sequence.

The general steps to create a template library in SeisCorr using a bulletin are:

1. Choose event origins from existing bulletin (e.g., SEL3 Origin table from IDC). This step creates a set of origin candidates for templates, and for convenience these origins are stored in an aftershock-specific Origin table.
2. Query to create a table of candidate template associations for the origins found in step 1.
3. Query to create a table of candidate template arrivals for the origins and associations found in steps 1 and 2.
4. Choose stations. For each station, follow steps 5 through 10.
5. Use SeisCorr to search for arrivals at the chosen station, using the candidate template events and candidate template associations, specifying the phase list and time boxing the arrival time.
6. Select a template window size and offset from the picked arrival time.
7. Choose a filter band based on the epicentral distance and filter the templates to enhance the signal.
8. Run an STA/LTA detector on all the templates in the library. Select an STA/LTA threshold, and discard candidate templates that do not meet the threshold. This step is optional if all the templates appear to have a good SNR.
9. Save candidate templates for the station as a library.
10. Set correlation coefficient threshold using the time-reverse method discussed earlier.

2.2.2. Correlation of Templates with Continuous Data

SeisCorr correlates each template from a template library across continuous waveform data for a specified time period. If the correlation score exceeds the template cross-correlation coefficient threshold, a single-station detection is recorded. Note that a correlation job must be run for every template library, and each template library represents waveforms from a single station. For 12 stations, for example, 12 correlation jobs would be required.

As previously mentioned, SeisCorr was implemented for historical data, not designed for use in a real-time system. A real-time waveform correlation system will have to process templates from many stations simultaneously over incoming waveform data; in contrast, SeisCorr is optimized to process many templates from a single station rapidly over historical waveform data. At the project launch meeting the decision was made to bypass the incorporation of SeisCorr algorithms into the real-time pipeline by defining a set of input and output database tables that can act as substitute steps for an algorithm. This approach allows us to use the interactive SeisCorr system on IDC data to develop template libraries, set thresholds and run correlations at SNL in our normal research environment, then deliver the template matches as an output database table that is analogous to the database arrival table for later use in the prototype pipeline being developed by the CTBTO.

2.2.3. Multistation Validation and Candidate Events

SeisCorr declares a detection when the correlation score from the correlation of the template with a waveform exceeds the template correlation coefficient threshold. A list of detections is produced as the template slides along the continuous data stream. We have found that waveform correlation finds many detections that cannot be validated with events in published bulletins. Often the events producing those detections are real, though their magnitudes are below the thresholds captured in the bulletins, but some of the detected events are false, despite the effort we put into screening templates and properly setting correlation thresholds for each template. Thus, SeisCorr includes an additional feature called multistation validation [3] that compares correlation detections across two

or more stations to look for detections that are -- in terms of location and time -- consistent with the same causal event. The location of a detection is assumed to be the location of the template event (i.e., the event from which the template waveform was recorded), while the origin time is calculated by subtracting the calculated travel time from the template event to the station. For multistation validation, SeisCorr clusters the detections from each station to improve the estimates of location and origin time for the common events. The SeisCorr user chooses distance and time tolerances to cluster the detections. Once a cluster of detections have been aggregated optimally relative to other clusters, SeisCorr calculates a location and origin time for the candidate event. The candidate events are delivered in the schema of the Origin table for later use in the prototype pipeline.

This subsection completes the overview of the features of SeisCorr. The remainder of the report will describe the specific use of SeisCorr for the aftershock project.

2.3. Template Libraries

A template library is a collection of templates for a single station. For this study, the approach to selecting the stations to use was modified based on intermediate results. The aftershock sequence associated with the April 2015 Nepal earthquake was the first sequence investigated because the authors have studied regional seismicity in this area and thus are familiar with the IMS stations near Nepal.

2.3.1. 2015 Nepal Template Libraries

Because the 2015 Nepal aftershock sequence was the first one studied, there was some method discovery that was required to adjust the typical approach to building template libraries to the specific problem of aftershock sequences. The 2015 Nepal mainshock, also known as the Gorkha earthquake, occurred on April 25, 2015 at 06:11:26 UTC time. The magnitude M_w 7.9 event was located at 28.13°N, 84.72°E and a depth of 13.4 km. The ISC event ID [6] for the 2015 Nepal earthquake is 607208674 [7].

Creating the 2015 Nepal template libraries:

1. The bulletin SEL3 was queried for events that occurred within 3 degrees radius from the mainshock epicenter and within the timespan from 1 week before the mainshock to 12 hours after the mainshock, resulting in 91 candidate template events for the aftershock sequence. The locations of the candidate template events and the locations of the REB events that we would like to detect with those templates are shown in Figure 2-3.

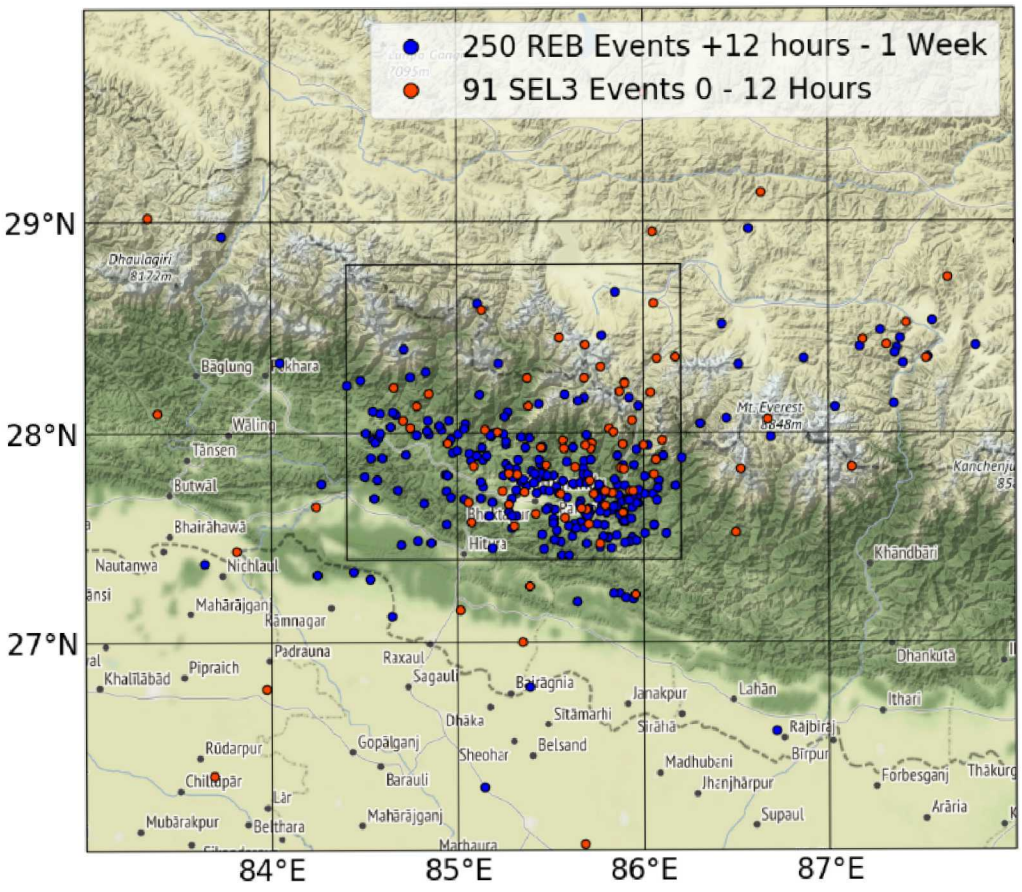

Figure 2-3. Locations of 2015 Nepal candidate template events from SEL3 (red) versus the locations of REB events for that sequence (blue). The black box indicates an area of focus that will be expanded in following maps of the 2015 Nepal aftershock sequence.

2. There were 5071 associations for the 237 origins queried from SEL3 for the timeframe of one week before the mainshock to one week after the mainshock. The two weeks of SEL3 origins were collected for later comparison with the REB events over the same timeframe.
3. There were 5071 arrivals queried for the origins and associations.
4. **Choosing stations for template libraries**. In an operational system that incorporates waveform correlation, it may be optimal to make template libraries for every station in the network that recorded an arrival for an event within the region of the aftershock. This was impractical for the funding granted for this research study, so a method of choosing stations was required to reduce the number of template libraries.

a. The initial approach to choosing the stations was based on discussion during the project launch meeting. Steven Gibbons, representing NORSAR, stated that he anticipated choosing the 3 to 5 stations with the most arrivals for the empirical matched field processing method [8]. Thus, our choice of stations was initially based on the number of stations with the most arrivals, and then the potential templates were created from arrivals that were seen by more than one station in that group. This approach did not work well because few potential templates chosen in this manner passed the STA/LTA screening for SNR. We reviewed potential templates and concluded that the arrays were operated with beam forming to magnify the teleseismic P signal from the aftershocks. This operational mode did not lead to templates with a high time-bandwidth product, which is preferred for waveform correlation. Thus, using the number of arrivals seen by a station as a factor for inclusion was abandoned as an approach for station selection.
b. The next approach to choosing stations was successful and was followed during the rest of the study. The stations were ordered by distance proximity from the epicenter of the mainshock, and the closest stations with the most phase (Pn, Pg, P) arrivals with a high average SNR were chosen for template libraries. The stations chosen for the 2015 Nepal sequence are reported in Table 2-2. There were other stations that may have been chosen using these criteria such as ARCES, NOA, TORD and YKA, but the collection of stations was limited to 13 due to funding.

Table 2-2. Stations for the 2015 Nepal event sorted in order of increasing epicentral distance.

Station	Distance (degrees)	Phase	Average SNR	# Origins	Station Name
CMAR	16.26	Pn	12.34	41	Chiang Mai, Thailand
		P	11.29	18	
MKAR	18.63	Pn	8.23	2	Makanchi Array, Kazakhstan
		P	34.45	76	
KURK	22.85	P	35.83	34	Kurchatov, Kazakhstan
GEYT	24.24	P	19.59	26	Alibeck Array, Turkmenistan
ZALV	25.69	P	31.1	69	Zalesovo Array, Russian Federation
SONM	25.81	P	36.54	61	Songino, Mongolia
KSRS	37.13	P	14.78	37	Camp Long, South Korea
USRK	40.74	P	18.18	28	Ussuriysk Array, Russian Federation
NRIK	41.17	P	25.94	47	Norilsk, Russian Federation
FINES	50.71	P	40.33	59	Finess Array, Finland
WRA	67.77	P	42.46	68	Warramunga Array, Australia
ASAR	70.06	P	32.2	66	Alice Springs Array, Australia
ILAR	79.03	P	26.69	48	Eielson, Alaska, USA

The steps 5-10 are performed for each station to create a template library.

5. For each station, Pn, Pg, and P phase arrivals were searched for each event within 3.0 degrees of the mainshock epicenter location for the time period between April 25, 2015 06:11:25 and April 25, 2015 18:00:00 UTC to make a 12-hour template library.
6. For the 2015 Nepal aftershock sequence, templates of different lengths were explored, such as 30 seconds, 20 seconds, and 15 seconds. The final choice for a template length of 15 seconds with an offset of 2 seconds before the arrival time was based on the concern that longer time windows could include multiple aftershocks. SeisCorr currently requires that all templates within a template library must have the same template duration.

NOTE: The template length for aftershock sequences could be explored in more depth in future research, possibly the use of template-specific lengths.

---

7. For the 2015 Nepal aftershock sequence, all the templates were filtered with a 3-pole Butterworth bandpass filter of 0.8–3.5 Hz.
8. The STA/LTA threshold screening was used on the 2015 Nepal template libraries to remove templates that did not have high enough SNR. The following parameters were used for the STA/LTA screening:
   a. Short-term average window = 1 second
   b. Long-term average window = 30 seconds
   c. Gap between windows = 0 seconds
   d. Minimum STA/LTA threshold was 3.0 for most of the template libraries. For ASAR and NRIK, the minimum STA/LTA threshold was 4.0. For ILAR, the minimum STA/LTA threshold was 5.0. The highest STA/LTA threshold above 3.0 was chosen that retained at least 80% of candidate templates.
9. The candidate templates that passed the STA/LTA threshold screening were saved as a template library. Figure 2-4 shows the number of templates for each station (i.e., library).

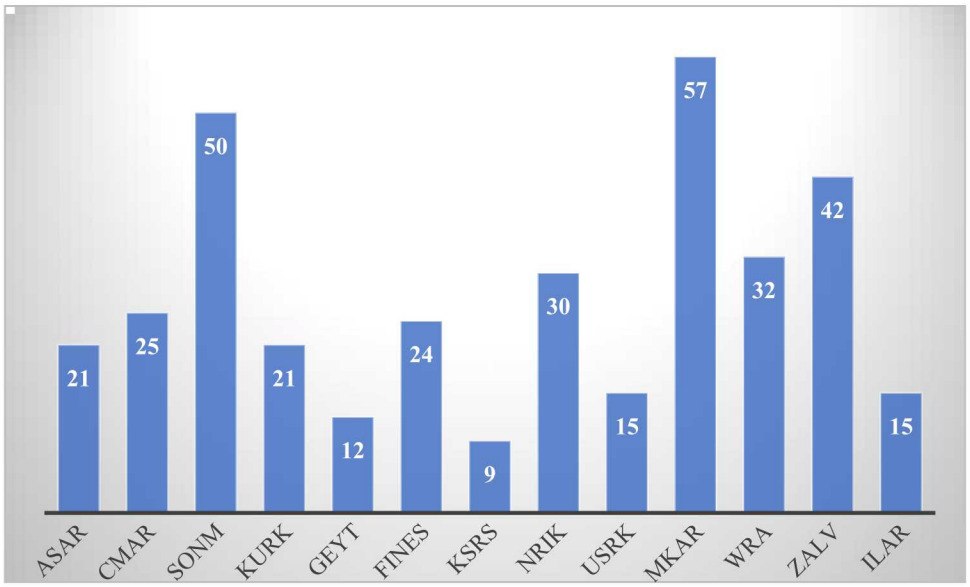

Figure 2-4. 2015 Nepal template count by station.

10. The template correlation coefficient thresholds were set using the time-reverse method, where the false alarm rate (FAR) was set to 1 FA per year. The templates were reversed and correlated against the background data from April 18, 2015 through May 3, 2015, encompassing a week of normal background noise and the week after the mainshock. As discussed above, the week after the mainshock was included to raise the noise level to include the aftershock sequence itself. After the threshold is calculated based on background noise, a small offset of 0.05 is added to the threshold value to raise the value beyond noise correlation values that were observed. The template threshold value statistics by station are shown in Figure 2-5, where the box extends from the lower to upper quartile of the threshold values with a line representing the median threshold value. The minimum (maximum) threshold value is the bottom (top) line of the distribution.

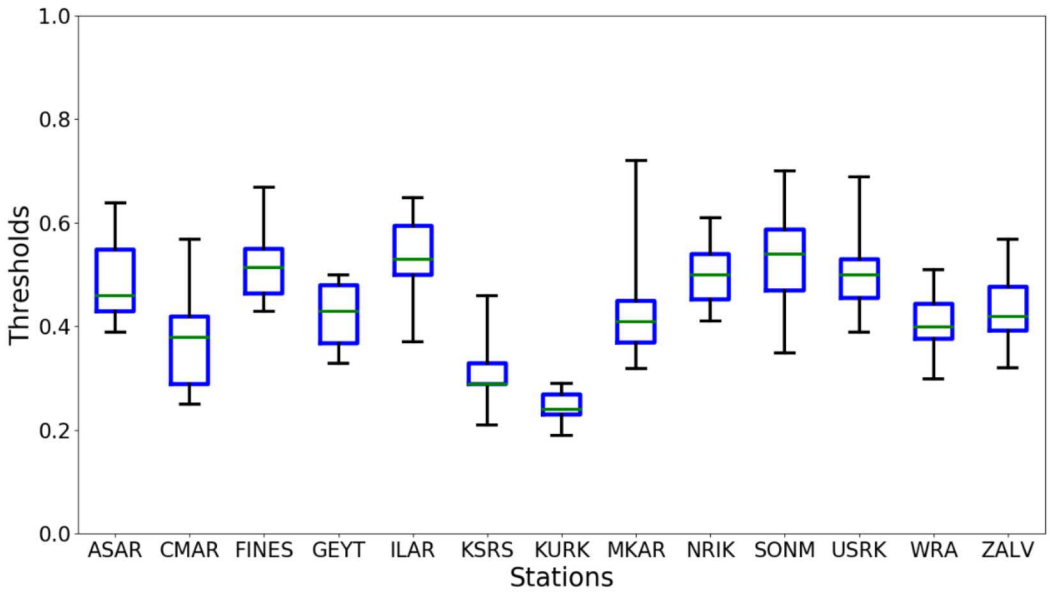

Figure 2-5. Statistics for 2015 Nepal template threshold values, alphabetical order by station.

The locations of the template events are shown in Figure 2-6, where each circle is both color-coded according to and proportional to the number of reporting stations. White circles indicate locations of events for SEL3 candidate templates that did not become templates because they did not pass STA/LTA threshold screening. The extent of the map in Figure 2-6 is the focus area shown by the black box in Figure 2-3. From the first 12 hours of the 2015 Nepal aftershock sequence, 76 events resulted in 353 templates from 13 stations.

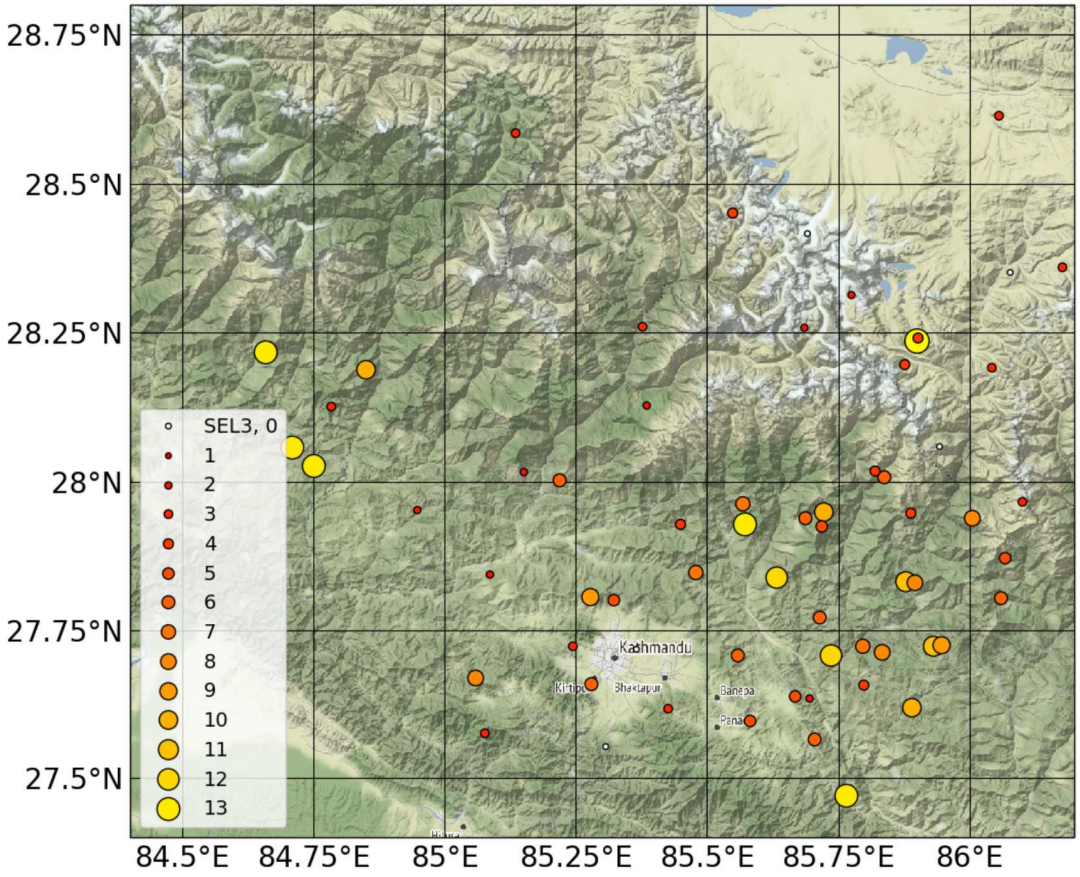

Figure 2-6. Locations of 2015 Nepal template events, by number of reporting stations.

2.3.2. 2015 Chile Template Libraries

The method for studying the 2015 Nepal aftershock sequence was carried forward and applied to the 2015 Chile aftershock sequence with few changes. The 2015 Chile earthquake, known as the 2015 Illapel earthquake, occurred on September 16, 2015 at 22:54:30 UTC time. The M_w 8.2 event was located at 31.64°S, 71.69°W, and a depth of 12.1 km. The ISC event ID [6] for the 2015 Chile earthquake is 611531714 [7].

Creating the 2015 Chile template libraries:

1. The event origins were queried from SEL3 within a box extending from 28°S to 34°S in latitude, and 71°W to 75°W in longitude, and within a timespan from 1 week before the mainshock to 12 hours after the mainshock, resulting in 88 candidate template events. The location of the

candidate template events versus the locations of the REB events that we would like to detect with the templates are shown in Figure 2-7.

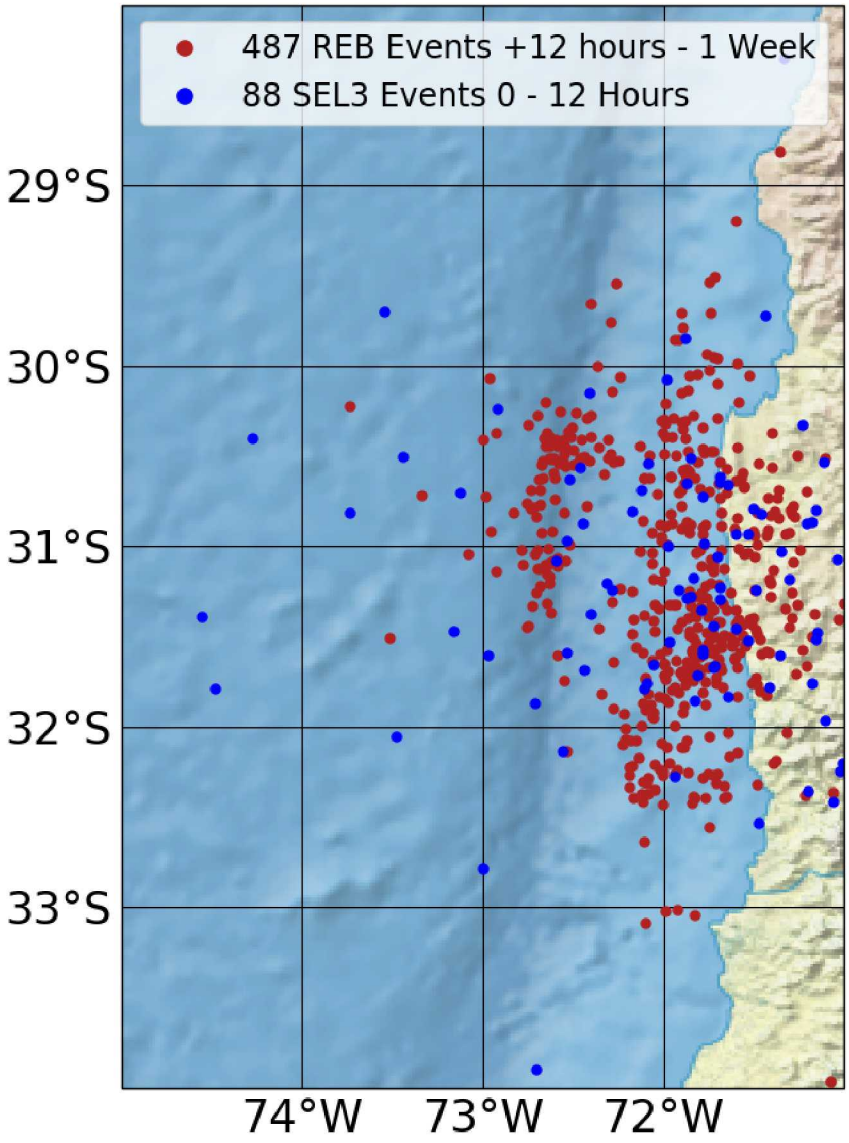

Figure 2-7. Locations of 2015 Chile candidate template events from SEL3 (blue) versus the locations of REB events from the aftershock sequence (red).

2. There were 9752 associations for 341 origins queried from SEL3 for the timeframe of one week before the mainshock to one week after the mainshock. The two weeks of SEL3 origins were collected for later comparison with the REB events over the same timeframe.
3. There were 9752 arrivals queried for the origins and associations.
4. **Choosing stations for template libraries**.

a. The stations were ordered by distance proximity from the epicenter of the mainshock, and the closest stations with the most phase (Pn, Pg, P) arrivals with a high average SNR were chosen for template libraries. The stations chosen for 2015 Chile are shown in Table 2-3.

Table 2-3. Stations for the 2015 Chile event sorted in order of increasing epicentral distance.

Station	Distance (degrees)	Phase	Average SNR	# Origins	Station Name
PLCA	9.18	P	8.1	21	Paso Flores, Argentina
		Pn	22.03	43	
CPUP	13.58	P	6.1	15	Villa Florida, Paraguay
		Pn	6.77	20	
LPAZ	15.55	P	11.35	23	La Paz, Bolivia
		Pn	15.73	37	
USHA	23.37	P	9.09	8	Ushuaia, Argentina
BDFB	26.75	P	13.7	57	Brasilia, Brazil
VNDA	66.54	P	8.62	22	Dry Valley, Antarctica
TXAR	67.79	P	15.82	65	Texas, USA
DBIC	74.1	P	22.97	57	Dimbroke, Cote D'Ivoire
MAW	75.41	P	16.43	51	Mawson, Antarctica
BOSA	80.91	P	12.81	51	Boshof, South Africa
NVAR	82.08	P	14.31	56	Mina Array, Nevada
TORD	83.08	P	37.87	53	Torodi Array, Niger

The steps 5-10 are performed for each station to create a template library.

5. Pn, Pg, and P phase arrivals were searched for each station within a box where the latitude ranged between 28 to 34 degrees South, and the longitude ranged between 71 to 75 degrees West, and for the time period between September 16, 2015 22:54:00 and September 17, 2015 10:54:00 UTC to make a 12-hour template library.
6. A template window of 15 seconds was used for the 2015 Chile aftershock sequence.
7. The bandpass filters for the 2015 Chile aftershock sequence are summarized in Table 2-4. A 3-pole Butterworth filter was used for all stations.

Table 2-4. 2015 Chile bandpass filters by station.

Station	Bandpass (Hz)
PLCA	2.0-10.0
CPUP	2.0-10.0
LPAZ	2.0-10.0
USHA	1.0-4.0
BDFB	1.5-4.0
VNDA	0.8-3.5
TXAR	0.8-3.5
DBIC	0.8-3.5
MAW	0.8-3.5
BOSA	0.8-3.5
NVAR	0.8-3.5
TORD	0.8-3.5

8. STA/LTA threshold screening was used on the 2015 Chile template libraries to remove templates that did not have a good SNR. The typical STA/LTA values for the 2015 Chile template libraries are:

a. Short-term average window = 1 second

b. Long-term average window = 30 seconds

c. Gap between windows = 0 seconds

d. Minimum STA/LTA threshold was 3.0 for most of the template libraries. STA/LTA thresholds were not applied to stations PLCA, CPUP, and LPAZ, which were geographically close to the earthquake and visually exhibited clear signals.

9. The candidate templates that passed the STA/LTA threshold screening were saved as a template library. Figure 2-8 shows the number of templates by station (i.e., library) for the 2015 Chile aftershock sequence.

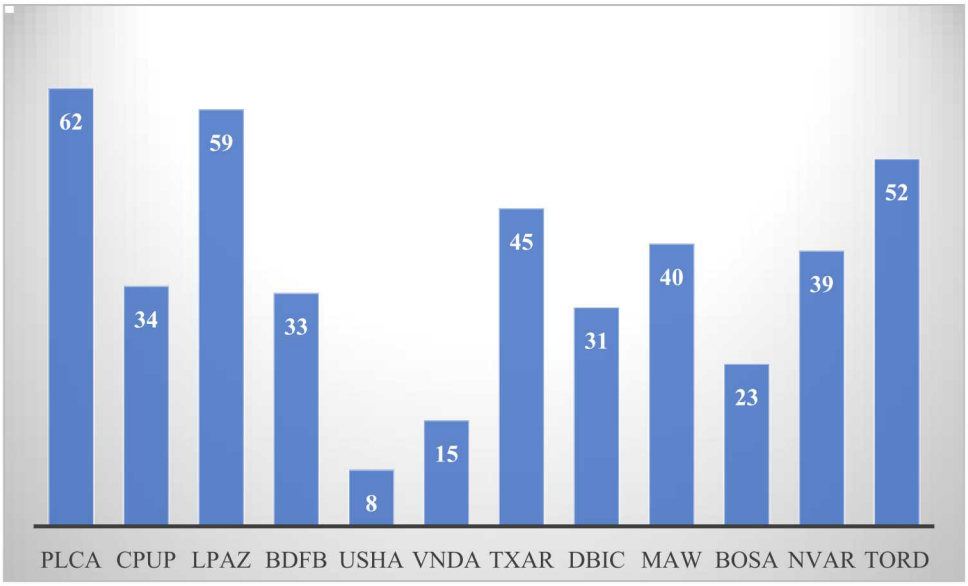

Figure 2-8. 2015 Chile template count by station.

10. The template correlation coefficient thresholds for the 2015 Chile templates were set using the time-reverse method, where the false alarm rate (FAR) was set to 1 FA per year. The templates were reversed and correlated against the background data from September 9, 2015 through September 23, 2015, encompassing a week of normal background noise and the week after the mainshock. The week after the mainshock was included to raise the noise level to include the aftershock sequence itself. After the threshold is calculated based on background noise, a small offset of 0.05 is added to the threshold value to raise the value beyond noise correlation values that were observed. The template threshold value statistics by station are shown in Figure 2-9, where the box extends from the lower to upper quartile of the threshold values with a line representing the median threshold value. The minimum (maximum) threshold value is the

bottom (top) line of the distribution.

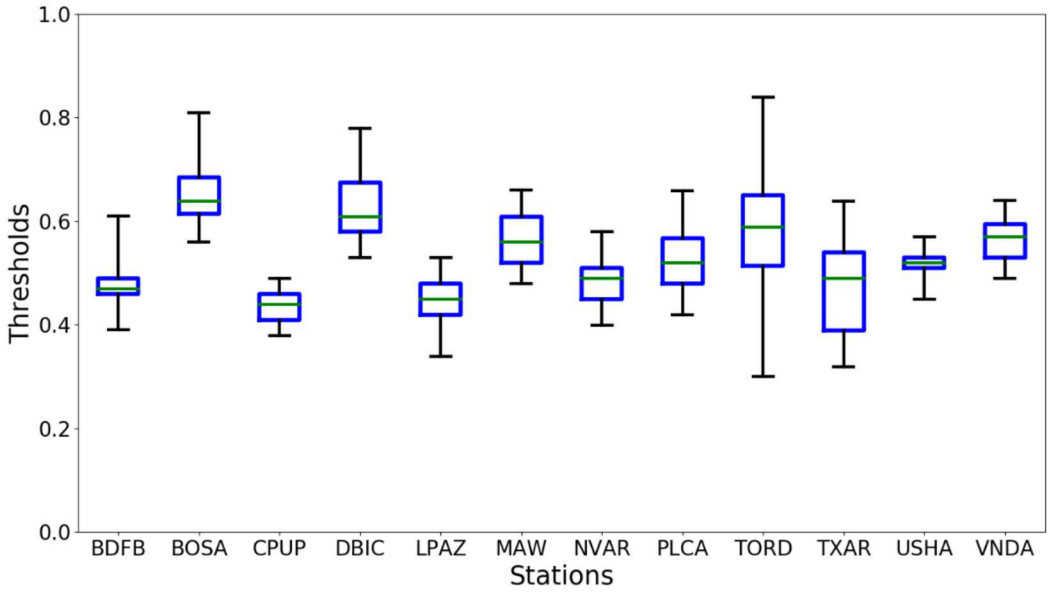

Figure 2-9. Statistics for 2015 Chile template threshold values, alphabetical order by station.

The locations of the 2015 Chile template events are shown in Figure 2-10, where each circle is both color-coded according to and proportional to the number of reporting stations. Black circles indicate locations of events for SEL3 candidate templates that did not become templates because they STA/LTA threshold screening. From the first 12 hours of the 2015 Chile aftershock sequence, 85 events resulted in 441 templates from 12 stations.

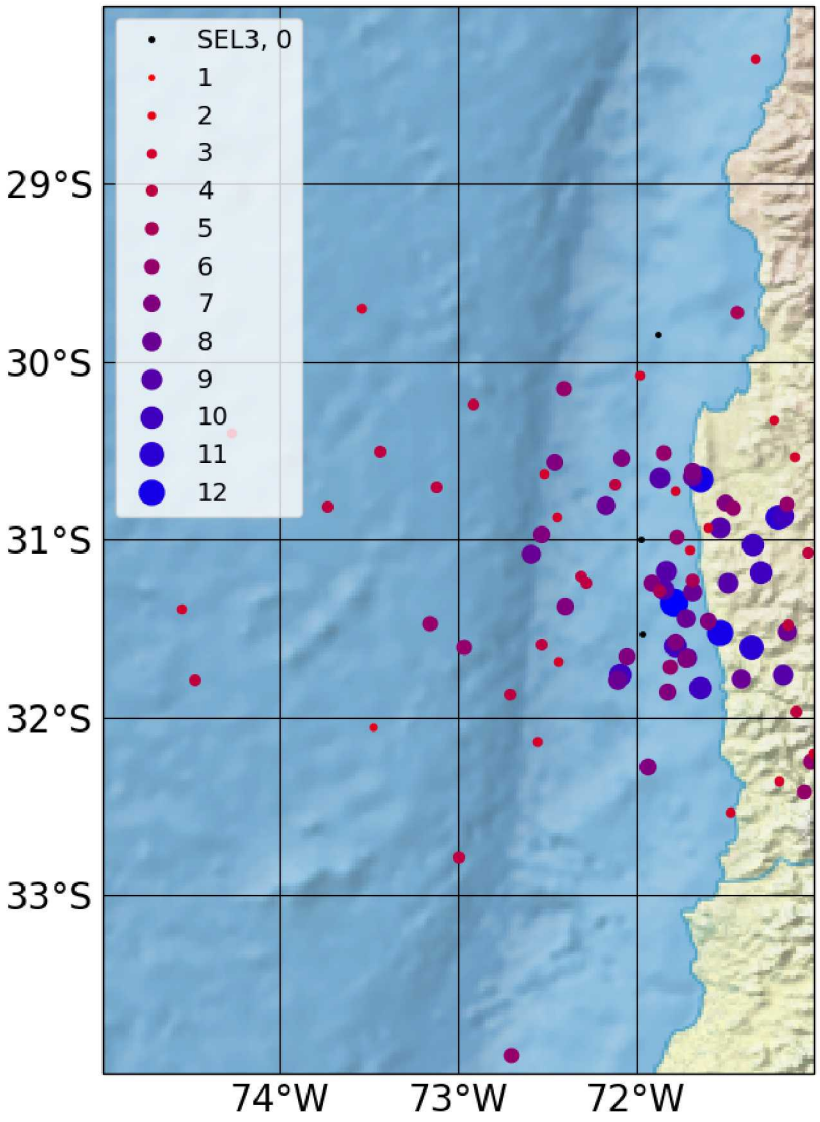

Figure 2-10. Location of 2015 Chile template events, by number of reporting stations.

2.3.3. 2011 Tohoku Template Libraries

The method for studying the 2015 Nepal aftershock sequence was carried forward and applied to the 2011 Tohoku aftershock sequence with few changes. The M_w (GCMT) 9.1 earthquake occurred on March 3, 2011 at 05:46:23 UTC time at 38.30°N and 142.50°E at a depth of 19.7 km. The ISC event ID [6] for the 2011 Tohoku earthquake is 16461282 [7].

Creating the 2011 Tohoku template libraries:

1. The event origins were queried from SEL3 within a box where the latitude ranged between 32 to 44 degrees North, and the longitude ranged between 140 to 146 degrees East, and within the timespan 1 week before the mainshock (in case of foreshocks) to 12 hours after the mainshock, resulting in 505 candidate template events for the aftershock sequence. The location of the

candidate template events versus the locations of the REB events that we would like to detect with the templates are shown in Figure 2-11.

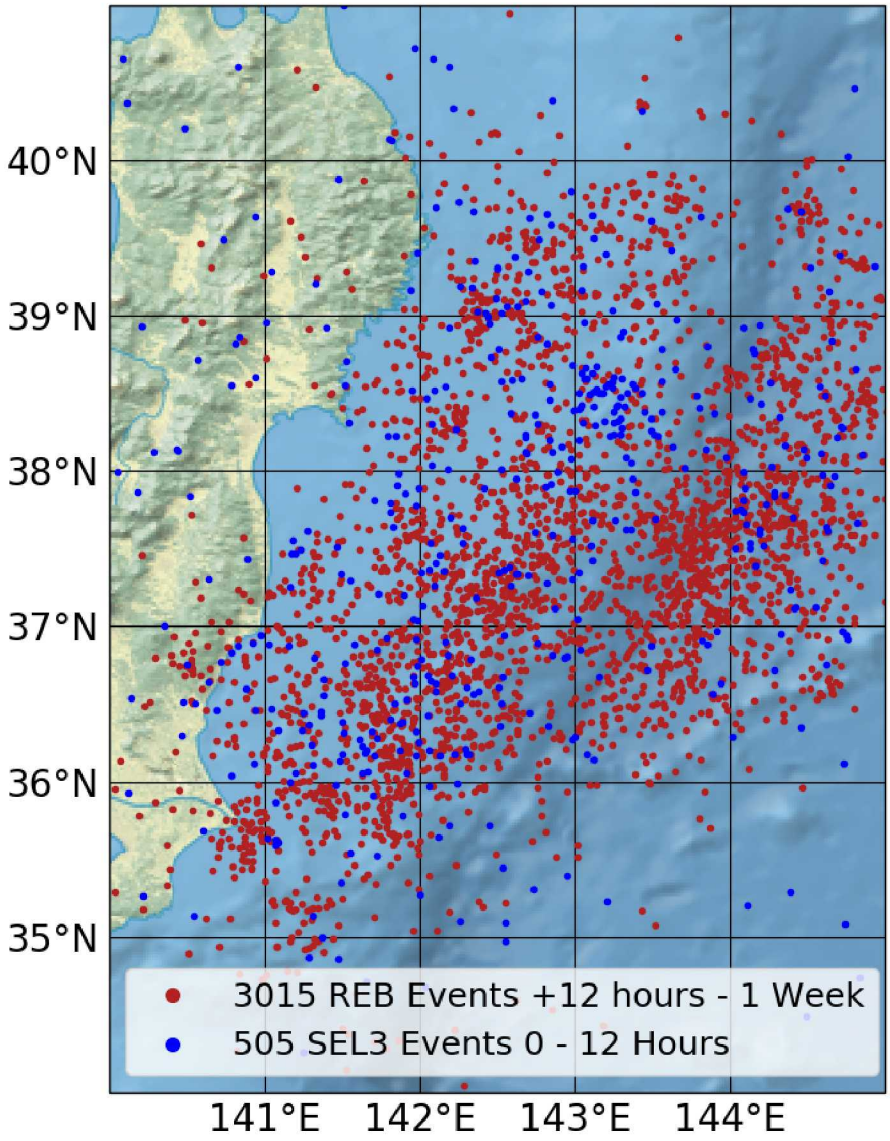

Figure 2-11. Locations of 2011 Tohoku candidate template events from SEL3 (blue) versus the locations of REB events from the aftershock sequence (red).

2. There were 80800 associations for 2839 origins queried from SEL3 for the timeframe of one week before the mainshock to one week after the mainshock. The two weeks of SEL3 origins were collected for later comparison with the REB events over the same timeframe.
3. There were 80800 arrivals queried for the origins and associations.
4. **Choosing stations for template libraries**.

a. The stations were ordered by distance proximity from the epicenter of the mainshock, and the closest stations with the most phase (Pn, Pg, P) arrivals with a high average SNR were chosen for template libraries. The stations chosen for 2011 Tohoku are shown in Table 2-5.

Table 2-5. Stations for the 2011 Tohoku event sorted in order of Increasing epicentral distance.

Station	Distance (degrees)	Phase	Average SNR	# Origins	Station Name
MJAR	3.76	Pn	34.53	135	Matsushiro Array, Japan
		Pg	12.51	47	
		P	35.61	123	
USRK	9.77	Pn	12.22	176	Ussuriysk Array, Russian Federation
		Pg	6.46	2	
		P	9.36	171	
KSRS	11.48	Pn	11.75	161	Camp Long, South Korea
		P	9.79	146	
SONM	27.72	P	20.77	253	Songino, Mongolia
ZALV	41.62	P	17.47	214	Zalesovo Array, Russian Federation
CMAR	42.56	P	11.92	167	Chiang Mai, Thailand
MKAR	44.09	P	22.77	94	Makanchi Array, Kazakhstan
ILAR	48.0	P	17.06	240	Eielson, Alaska, USA
ASAR	62.17	P	17.0	252	Alice Springs Array, Australia
YKA	62.31	P	12.91	200	Yellowknife Array, Canada
NOA	73.29	P	15.21	185	NORSAR Array, Norway
AKASG	73.74	P	22.1	209	Malin Array, Ukraine

The steps 5-10 are performed for each station to create a template library.

5. Pn, Pg, and P phase arrivals were searched for each station within a box where the latitude ranged between 32 to 44 degrees North, and the longitude ranged between 140 to 146 degrees East, and for the time period between March 4, 2011 05:46:00 and March 11, 2011 17:46:00 UTC to make a 12-hour template library that also includes foreshocks from the previous week.
6. A template window of 15 seconds was used for the 2011 Tohoku aftershock sequence.
7. The bandpass filters for the 2011 Tohoku aftershock sequence are summarized in Table 2-6. A 3-pole Butterworth filter was used for all stations.

Table 2-6. 2011 Tohoku bandpass filters by station.

Station	Bandpass (Hz)
MJAR	2.0-8.0
USRK	2.0-8.0
KSRS	1.0-8.0
SONM	1.0-4.0
ZALV	0.8-3.5
CMAR	0.8-3.5
MKAR	0.8-3.5
ILAR	1.0-3.0
ASAR	1.0-3.0
YKA	0.5-3.0
NOA	1.0-3.0
AKASG	1.0-3.5

8. STA/LTA threshold screening was used on the 2011 Tohoku template libraries to remove templates that did not have a good SNR. The typical STA/LTA values for the 2011 Tohoku template libraries are:

a. Short-term average window = 1 second

b. Long-term average window = 30 seconds

c. Gap between windows = 0 seconds

d. Minimum STA/LTA threshold was 3.0 for most of the template libraries. For ASAR, YKA, NOA and AKASG the minimum STA/LTA threshold was 4.0. For ILAR, the minimum STA/LTA threshold was 5.0.

9. The candidate templates that passed the STA/LTA threshold screening were saved as a template library. Figure 2-12 shows the number of templates by station (i.e., library) for the 2011 Tohoku aftershock sequence.

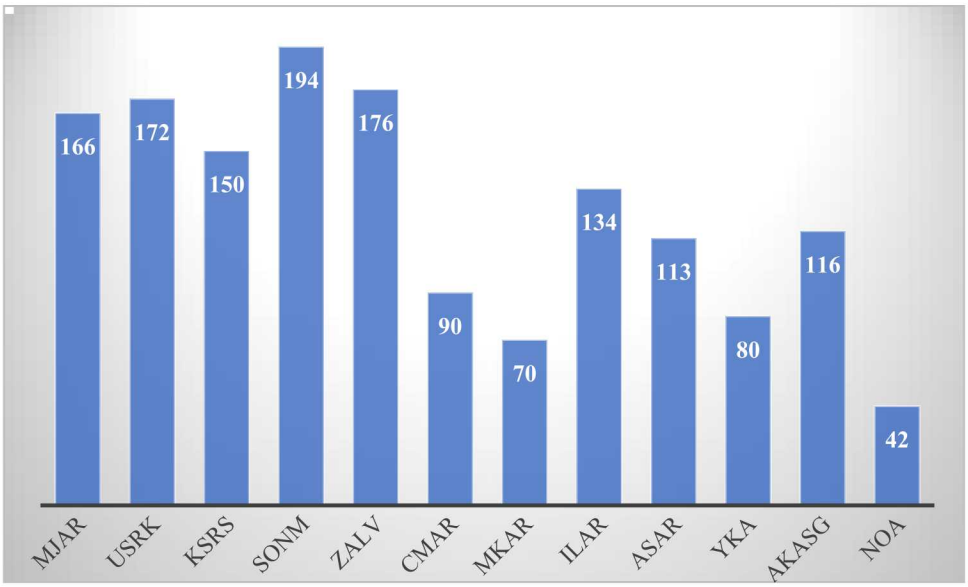

Figure 2-12. 2011 Tohoku template count by station.

10. The template correlation coefficient thresholds for the 2011 Tohoku templates were set using the time-reverse method, where the false alarm rate (FAR) was set to 1 FA per year. The templates were reversed and correlated against the background data from March 4, 2011 through March 18, 2011, encompassing a week of normal background noise and the week after the mainshock. The week after the mainshock was included to raise the noise level to include the aftershock sequence itself. After the threshold is calculated based on background noise, a small offset of 0.05 is added to the threshold value to raise the value beyond noise correlation values that were observed. The template threshold value statistics by station are shown in Figure 2-13, where the box extends from the lower to upper quartile of the threshold values with a line representing the median threshold value. The minimum (maximum) threshold value is the

bottom (top) line of the distribution.

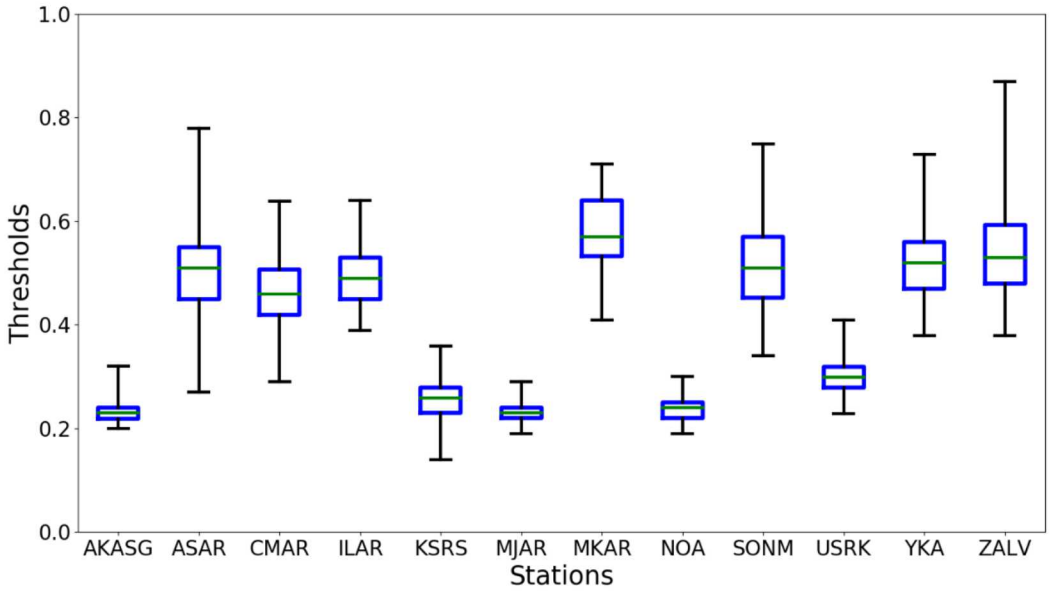

Figure 2-13. Statistics for 2011 Tohoku template threshold values, alphabetical order by station.

The locations of the 2011 Tohoku template events are shown in Figure 2-14, where each circle is both color-coded according to and proportional to the number of reporting stations by color and size of the circle. Black circles indicate locations of events for SEL3 candidate templates that did not become templates because the they did not pass STA/LTA threshold screening. From the first 12 hours of the 2011 Tohoku aftershock sequence and foreshocks, 389 events resulted in 1503 templates from 12 stations.

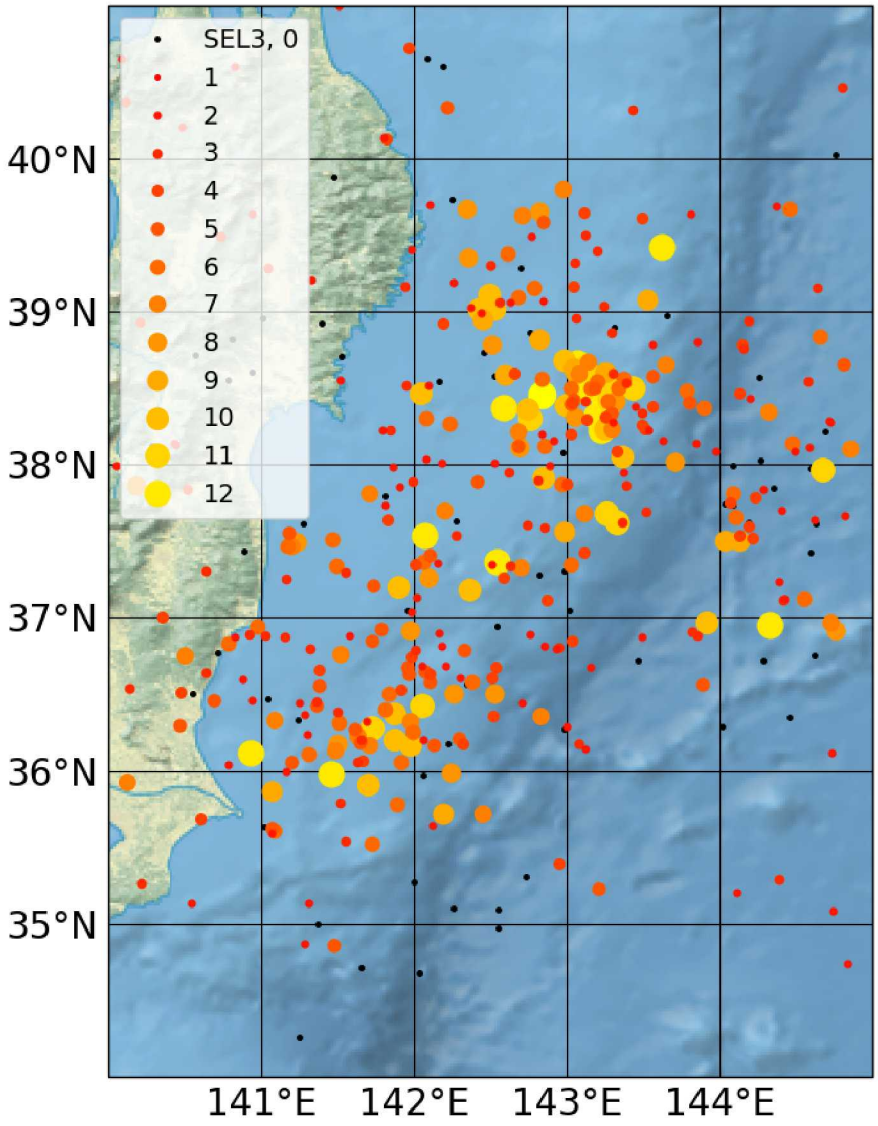

Figure 2-14. Location of 2011 Tohoku template events, by number of reporting stations.

2.4. Correlation Jobs

For each aftershock sequence, template waveforms in the template libraries are correlated against continuous waveform data from the same station to detect similar waveforms from aftershocks. Detections are recorded if the correlation score at a point in time exceeds the template correlation coefficient threshold.

NOTE: Future research could evaluate the effectiveness of templates by number of reporting stations. We believe that template events with larger numbers of reporting stations are likely to be better located; thus, we speculate that detections from these templates

will be more accurate. It would also be interesting to view the distribution of correlation scores to determine if detections with a high score are validated by multistation validation and compare well with REB bulletin events.

Table 2-7 shows a summary of the correlation jobs that were executed for each aftershock sequence, indicating the overall number of templates and detections.

Table 2-7. Summary of correlation jobs by aftershock sequence

Aftershock Sequence	Correlation Start	Correlation End	# Templates	# Detections
2015 Nepal	April 25, 2015 18:00:00 UTC	May 2, 2015 06:00:00 UTC	353	968
2015 Chile	September 17, 2015 10:54:00 UTC	September 23, 2015 22:54:00 UTC	441	960
2011 Tohoku	March 11, 2011 17:46:24 UTC	March 18, 2011 05:46:24 UTC	1503	24237

2.5. Multistation Validation

Multistation validation is a feature in SeisCorr that joins correlation detections that are coincident in origin time and location -- within a user-specified tolerance -- to form candidate events. Studies over broad areas under non-aftershock conditions can use tolerances on the order of 30 seconds and 150 km because seismicity is typically sparse in location and time. For a network, multistation validation can significantly reduce the overall false alarm rate if the requirement that an event is declared only if it is detected by multiple stations in the network is applied.

Yet aftershock sequences pose a particular challenge because the events are close together. The problem is exacerbated if the network is global and sparse, like the IMS, because the locations may be poorly resolved. The result is that it is difficult to resolve the locations sufficiently to use a location tolerance to separate aftershock events, thus the time tolerance becomes the crucial discriminant to separate aftershock events, though this is also problematic because aftershock events can occur within seconds of each other. This study used a multistation validation method that has been extended for aftershock events. Using the 2015 Nepal sequence, we parameterized the time and location tolerances to determine what tolerance values formed the most credible candidate events. Once the tolerances were determined for the 2015 Nepal sequence, a similar approach was employed to choose tolerances for the other aftershock sequences.

NOTE: Future research could investigate whether every aftershock sequence requires parametric analysis to set tolerances for multistation validation, or if standard tolerances can be justified.

Section 2.5.1 presents some example candidate events produced by multistation validation to develop intuition about the SeisCorr method. Section 2.5.2 describes the parameterization study of the 2015 Nepal aftershock sequences used to select the tolerance values. The following sections will analyze the candidate events for each of the three aftershock sequences using the tolerances.

2.5.1. Example candidate events

The purpose of this section is to develop an intuition about the way that SeisCorr uses multistation validation to join correlation detections into candidate events. The correlation jobs for all the stations must be completed prior to running a multistation validation job. The user specifies what correlation jobs to include in a multistation validation job and what distance and time tolerances to use to search for candidate events.

Figure 2-15 shows an example candidate event from the 2015 Nepal aftershock sequence that was detected by templates from 6 stations, superimposed over the map of the template events. The underlying map of template events is the same as Figure 2-6, and is shown here to indicate the locations of the detecting template events as well as the locations of all the template events, and to provide the scale for the clustered detections.

The legend indicates information about both the template event and the detection for each detecting template. The template event is the event from which the template waveform was recorded. In the case of this example, four of the templates (1, 2, 4, and 6) are waveforms from the mainshock; i.e., all four template events are the same earthquake recorded by different stations.

In SeisCorr, the location of the candidate event is estimated using an algorithm that averages over the locations of the events for the detecting templates. The location of the candidate event is indicated in Figure 2-15 by a white star, and the calculated origin time of the candidate event is indicated in the legend. The location calculated for the candidate event is heavily weighted towards the location of the majority of the detecting templates for this event, which places it near the location of the mainshock.

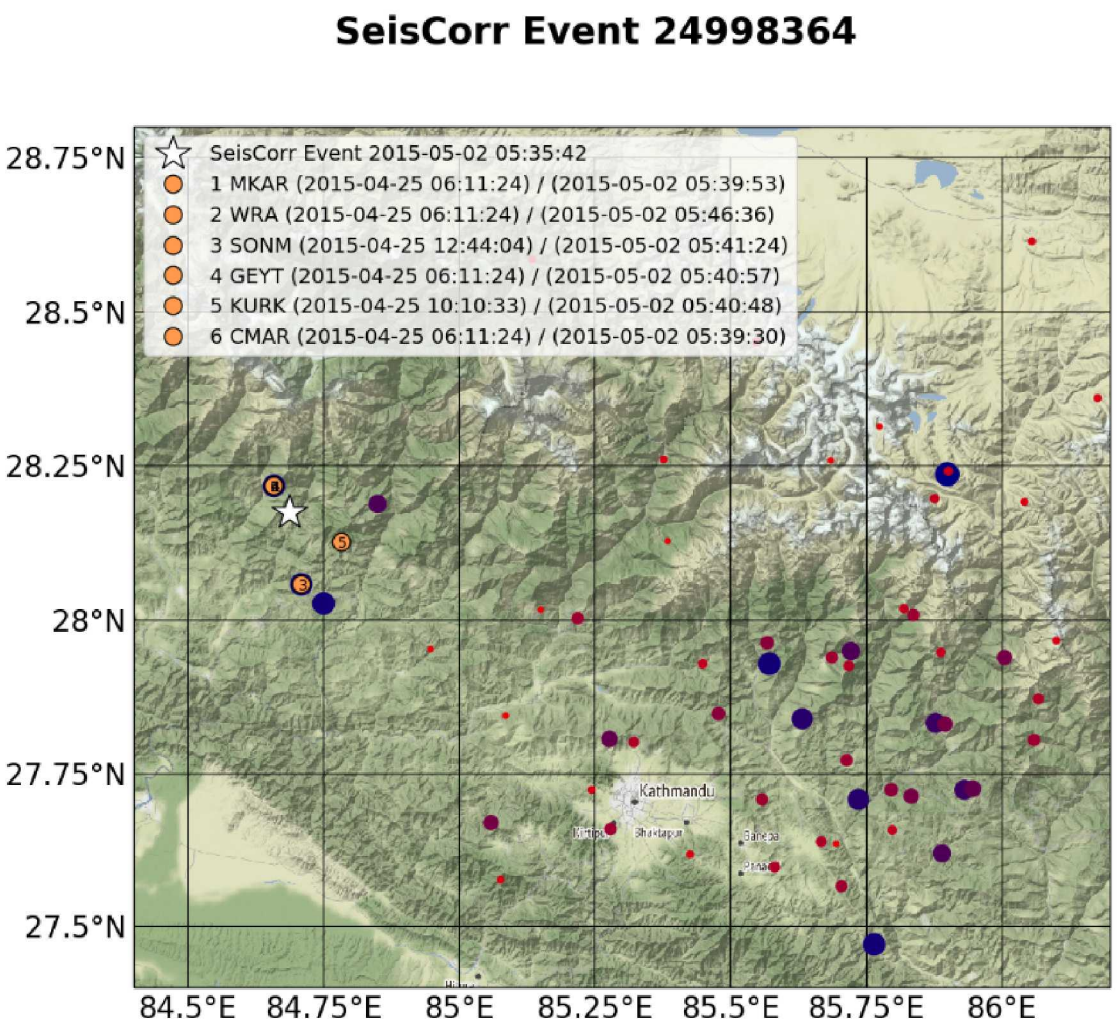

Figure 2-15. Example candidate event created from SeisCorr using multistation validation with tolerances of 100 km and 15 seconds. The candidate event location and time (UTC) is associated with the white star. The legend indicates the template station, template event date/time (UTC), and detection date/time (UTC), and a number chosen for convenience to label the location of the template on the map. This example candidate event was detected by four mainshock templates from stations MKAR (1), WRA (2), GEYT (4), and CMAR (6) that have the same location and time. The other two detecting templates from SONM (3) and KURK (5) are from nearby locations but the templates were from events later in the 12-hour aftershock sequence.

A second example candidate event is shown in Figure 2-16. The map shows the locations of the candidate event and template events for an event detected by three templates. As would be expected, the event location is nearly equidistant from the three detecting template events.

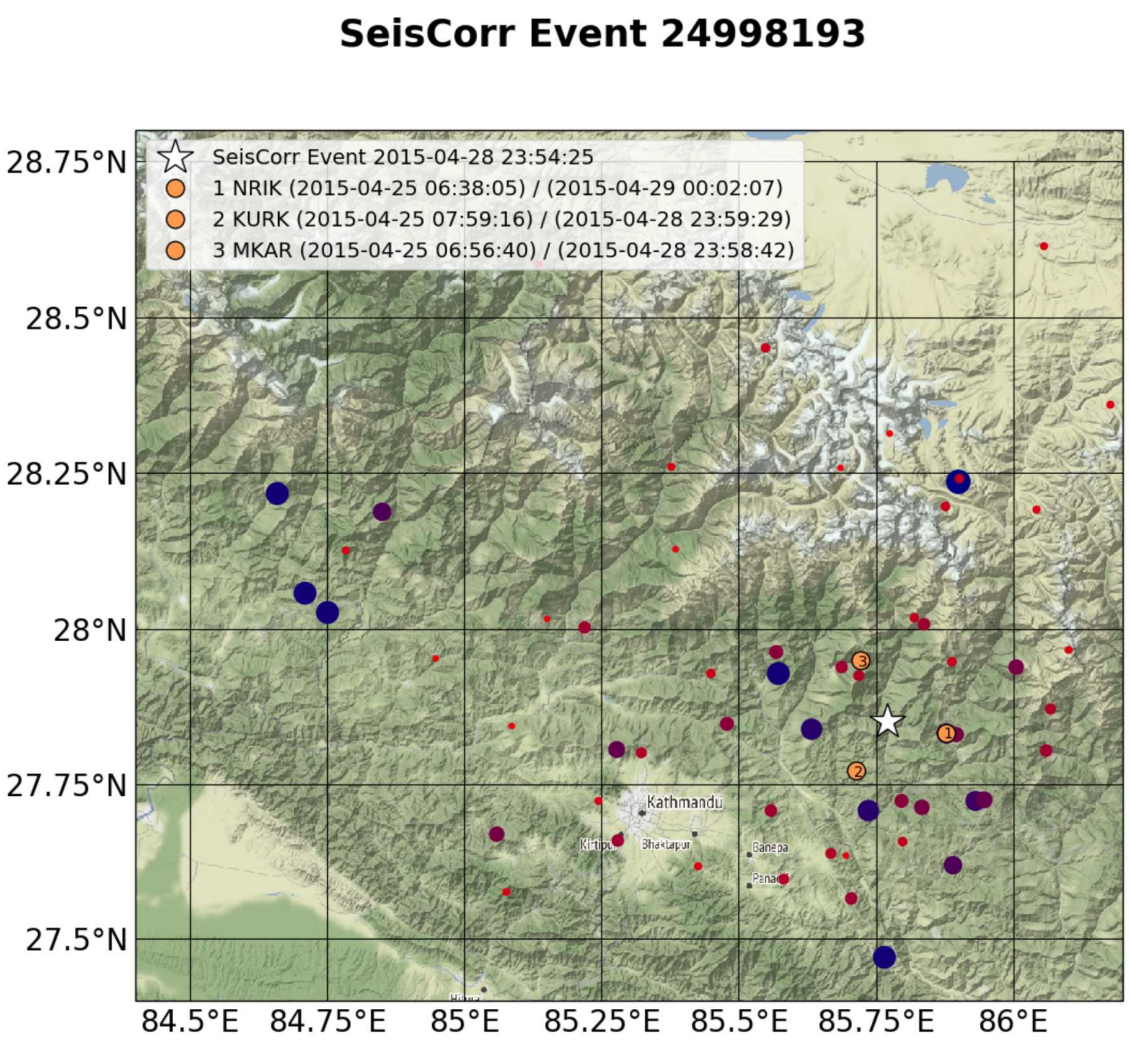

Figure 2-16. Analogous to Figure 2-15. This candidate event was detected by three templates.

Figure 2-17 displays example waveforms for the candidate event in Figure 2-16. For an array with many elements, such as KURK, it is possible to see a moveout across the array for both the templates and matching waveforms, which increases confidence in the detection. Note that the array KURK has a correlation score of 0.479, which is similar to that of the three-component station NRIK. However, our experience with waveform correlation indicates that array detections are more reliable than three-component detections due to the additional requirement for array stations that waveform moveout must match to exceed the correlation threshold.

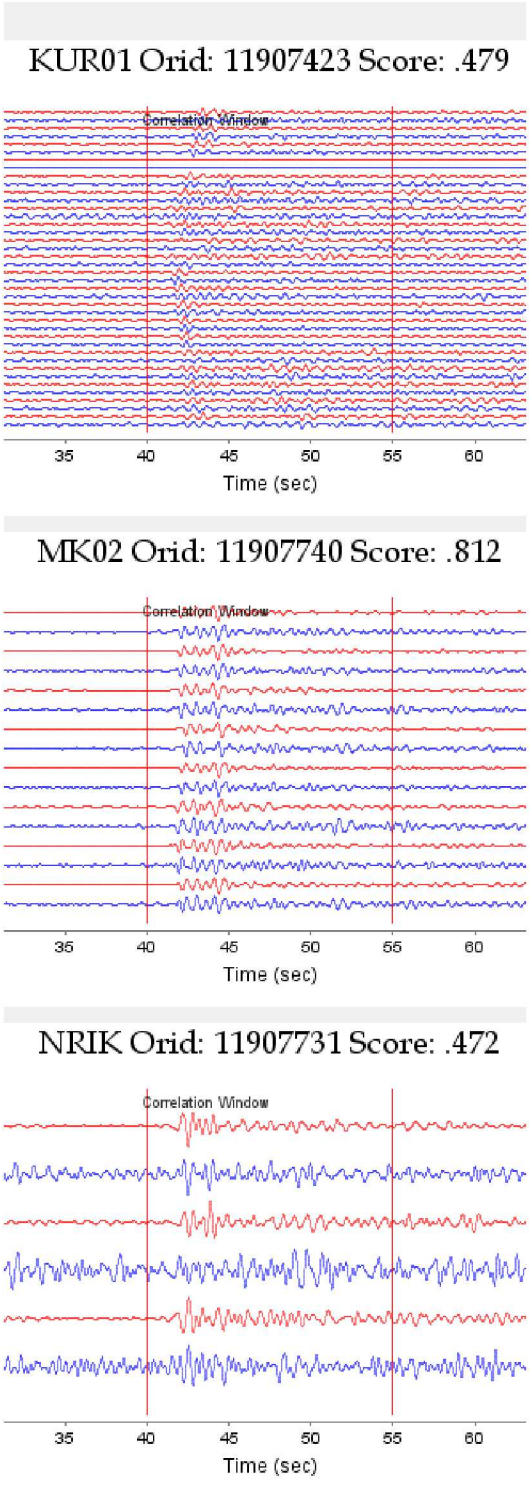

Figure 2-17. Waveforms for example candidate event 24998193 (map in Figure 2-16). For each detecting station, the template origin identifier and correlation score are shown above the waveform plot. The template waveforms are shown in red, with red vertical bars indicating the 15-second wide correlation window. The matching waveform is shown in blue.

NOTE: The IDC plans to incorporate waveform correlation into a prototype automated pipeline that generates correlation detections above thresholds, but an associator (e.g., NET-VISA [9]) will build events by associating the correlation detections to the events from the standard event lists. The authors encourage the IDC to consider a display of correlation templates and detections in a manner that will allow analysts to easily include those detections when they are credible or discard them when they are dubious.

The goal of this section was to introduce the way that SeisCorr uses template detections in multistation validation to detect candidate events. The examples should motivate the reader for the next section, where a method for estimating tolerances to use for multistation validation for aftershock sequences is prototyped and explained.

2.5.2. Parameterization study of time/location tolerances

SeisCorr has been used to study regional seismicity, where events are sparse in distance and time, and for aftershocks where the station spacing is adequate to separate the events in time. This research was the first study of aftershock events using SeisCorr with IMS stations alone; moreover, the use of the automatic SEL3 bulletin increases the inaccuracies in template event location. It was necessary to study the results of candidate events from multistation validation to understand what tolerances would optimize the detection of credible aftershocks that are close in distance and time relative to the stations in the global network.

As described in the previous section, spatial and temporal tolerances are required for multistation validation. Using the same group of correlation jobs for the 2015 Nepal sequence, the tolerances were varied to explore the values at which different events would begin to combine (tolerances too loose) or single events would split (tolerances too tight). 144 multistation validation jobs were run to infer optimum distance and time tolerances. The template libraries described in 2.3.1 2015 Nepal Template Libraries were correlated against continuous data from the first 12 hours of the aftershock sequence, guaranteeing that every template detect at least one event (the template event) and ensuring a population of events with very high correlation scores.

Let us first examine likely real events by choosing only events that have been validated by 3 or more stations and have average cross-correlation scores greater than 0.8. The number of events during the first 12 hours of the 2015 Nepal aftershock sequence that meet these stringent criteria are reported in Figure 2-18 against the tolerance values. This graph shows fundamental characteristics that are different from results we have observed for regional studies. The interesting features are:

1. As the distance tolerance is decreased from 150 km to 25 km for time tolerances of 50 s (blue) and 30 s (orange), the number of events increases. Typically, the number of events decreases as the distance tolerance decreases for regional studies because fewer event candidates are validated/confirmed by multistation validation. We postulate from this difference exhibited by aftershock data that a distance tolerance that is too large will combine distinct events, resulting in an overall decrease in the event count.
2. The green line represents events where all the detections are within 1 second, which is an unrealistic tolerance. Moreover, even when the distance tolerance is reduced to a value as low as 1 km, the number of events remains constant. We believe that the 40 events for the green line are detected by templates that share the same template event; that is, we could reduce the tolerances to an arbitrarily small distance and time and these events would

remain. This gives an estimate of the absolute minimum number of events that are required, and any combination of tolerances that result in fewer events are less than optimum.

3. As the time tolerance is decreased from 30 s (orange) to 10 s (grey), the number of events increases for all distance tolerances above 10 km. We postulate that this indicates that any time tolerances of 10 s or less are too tight and the real events are split into multiple events.

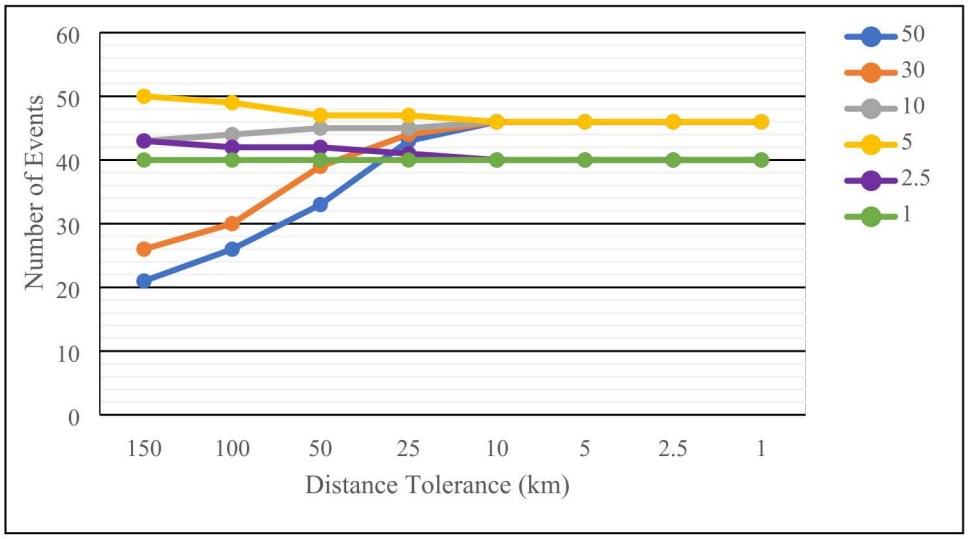

Figure 2-18. Number of events that have been validated by 3 or more stations during the first 12 hours of the 2015 Nepal aftershock sequence with average cross-correlation scores greater than 0.8 over a range of time and distance tolerances. The time tolerance in seconds is indicated by the line color.

Although Figure 2-18 offers interesting insights, it does not provide a view of the data that is complete enough to choose tolerances. Rather, it helps to set a minimum value on time (10 s) and suggests that 30 s is too loose a time tolerance, resulting in combined events. Moreover, we discovered that too large a distance tolerance will lead to combined events, as shown by the gap between the minimum of 40 events set by the 1 s (green) line and the 30 s (orange) and 50 s (blue) lines, but there is insufficient information to choose a distance tolerance from this graph alone.

Next, we examine all the three-station events, this time including events based on any correlation scores above the template cross-correlation coefficient threshold (Figure 2-19). A mix of combined events and split events are expected as the tolerances vary. The important indicators on this figure are enumerated below:

1. The increase in the number of events on the 50 s (blue) line as the distance tolerance decreases from 150 km to 100 km is interpreted as events that are combined at the larger distance tolerance. This sets a maximum distance tolerance somewhere between 100 and 150 km.

2. For all time tolerances, the number of events decreases for distance tolerances less than 100 km. We use this observation to choose a distance tolerance of 100 km for the multistation validations. While this distance tolerance value may include some combined events, reducing the tolerance even more splits larger numbers of events regardless of the time tolerance.

3. Finally, the observation that the 30 s (orange) time tolerance line is unchanged between the 150 km and 100 km distance tolerance to indicate that events are not combined or split at

this time tolerance value. In contrast, the 10 s (gray) line shows a decrease in number of events for all distance tolerances, leading to the conclusion that 10 s is too tight a tolerance. During the multistation validation runs over the entire aftershock sequence, it was discovered that a compromise time tolerance of 15 s performed better than tolerances of 30, 20, 12, and 10 s for two reasons:

a. The templates are 15 s in duration, and this duration was chosen based on observing the frequency of overlapping events during the first 12 hours of the aftershock sequence,

b. In combination with a 100 km distance tolerance, a 15 s time tolerance reduced the number of observed combined events in Figure 2-18 and also reduced the number of split events indicated by Figure 2-19.

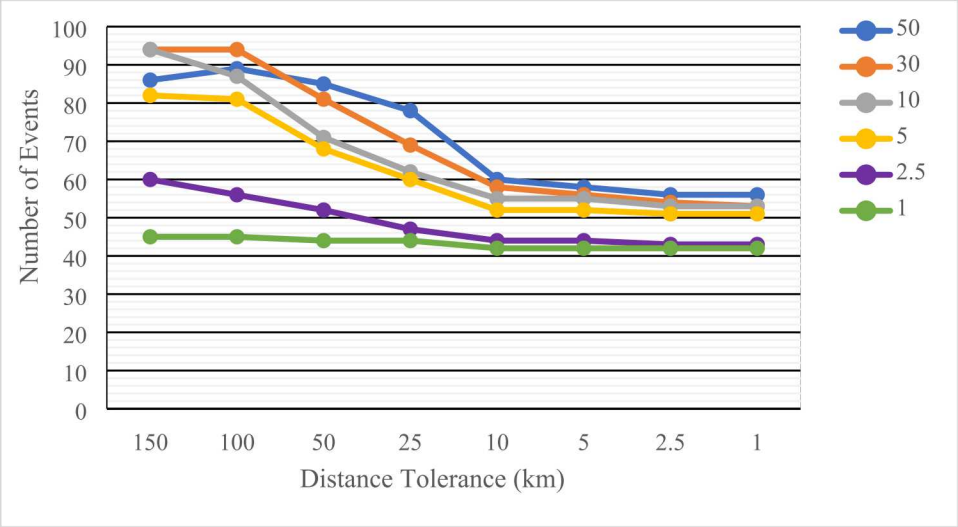

Figure 2-19. Number of events that have been validated by 3 or more stations during the first 12 hours of the 2015 Nepal aftershock sequence over a range of time and distance tolerances. The time tolerance (seconds) is indicated by the line color.

Based upon the analysis of discrete values in the parameterized study described in this section and further experimentation using the full aftershock sequence, the multistation validation tolerances chosen for the 2015 Nepal aftershock sequence are 100 km and 15 s for distance and time, respectively.

NOTE: Further research may be required in this area to optimize time and distance tolerances for aftershock events detected with waveform correlation in the context of a global network, even in combination with a sophisticated associator. This study offers some insights into the problem of balancing combining events with tolerances that are too large versus splitting events with tolerances that are too tight.

2.5.3. 2015 Nepal Events

The locations of events detected by waveform correlation for the 2015 Nepal aftershock sequence are shown in the map (Figure 2-20). The size and color of the circle indicates the number of detecting templates, which usually corresponds to the number of detecting stations. However, in some cases an event can be detected by two templates from two different phases recorded at the

same station (e.g., Pn and P). There were 597 distinct events confirmed by multistation validation using the tolerances of 100 km and 15 s for the 13 IMS stations listed in Table 2-2; 182 of the 597 events were detected by two or more stations. A few events were located outside of the map extent and are not shown in this figure. This map includes single station events, where a detection was made by one template but there were no other validating templates within the chosen tolerance. In the case of a single station event, the location is assumed to be the location of the template event.

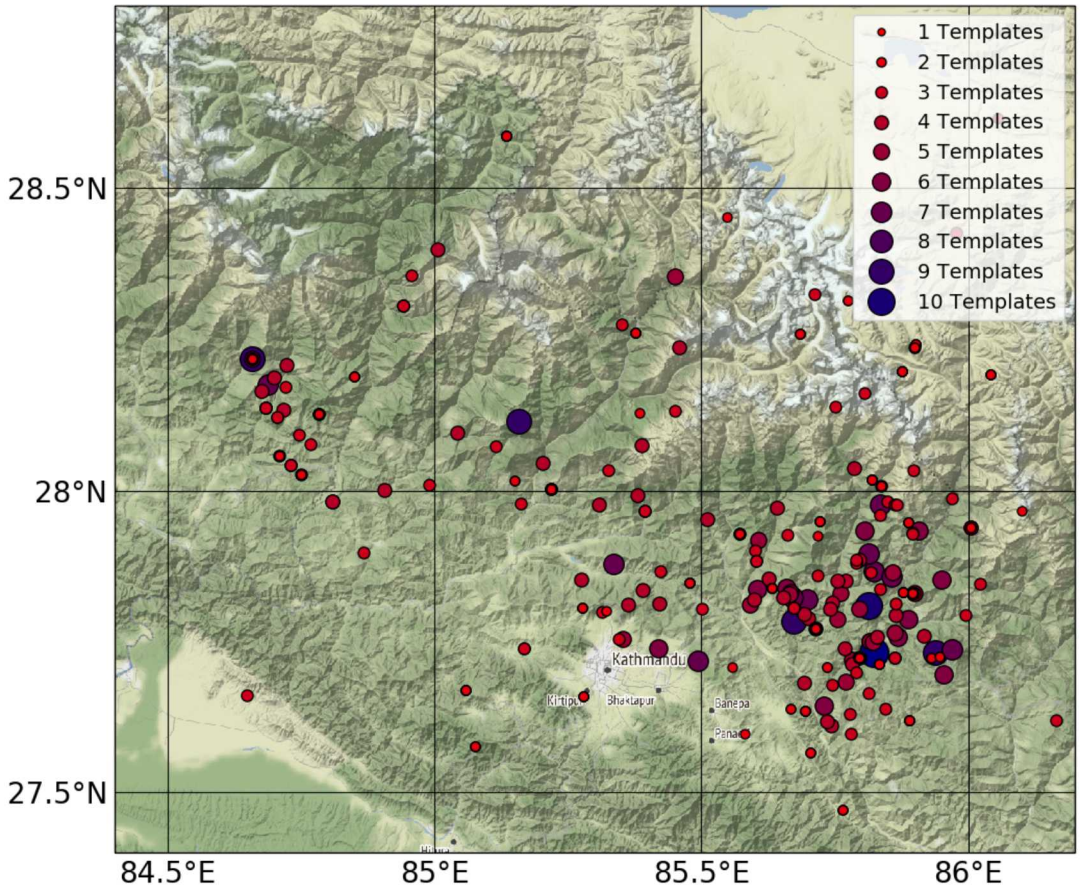

Figure 2-20. Map showing the locations of the 597 aftershocks for the 2015 Nepal sequence detected by waveform correlation. The size and color of the circle indicates the number of detecting templates.

The bar chart in Figure 2-21 shows the count of events over 12-hour increments, spanning the entire week of the study of the 2015 Nepal aftershock sequence. The first 12 hours includes the REB events (orange), SEL3 events (green) and the templates that were created from the SEL3 candidate events. The IDC analysts added many events manually because the number of REB events far exceeds the number of SEL3 events. This fact is shown directly by comparing the number of REB events that match SEL3 (red), where the location and time must be within a radius of 1 degree and ±15 s to declare the origins the same. After the first 12 hours, the remaining increments have two more additional bars that indicate the number of events detected by waveform correlation (blue) and the number of REB events that match waveform correlation events (yellow) within the tolerances of 1 degree and ±15 s.

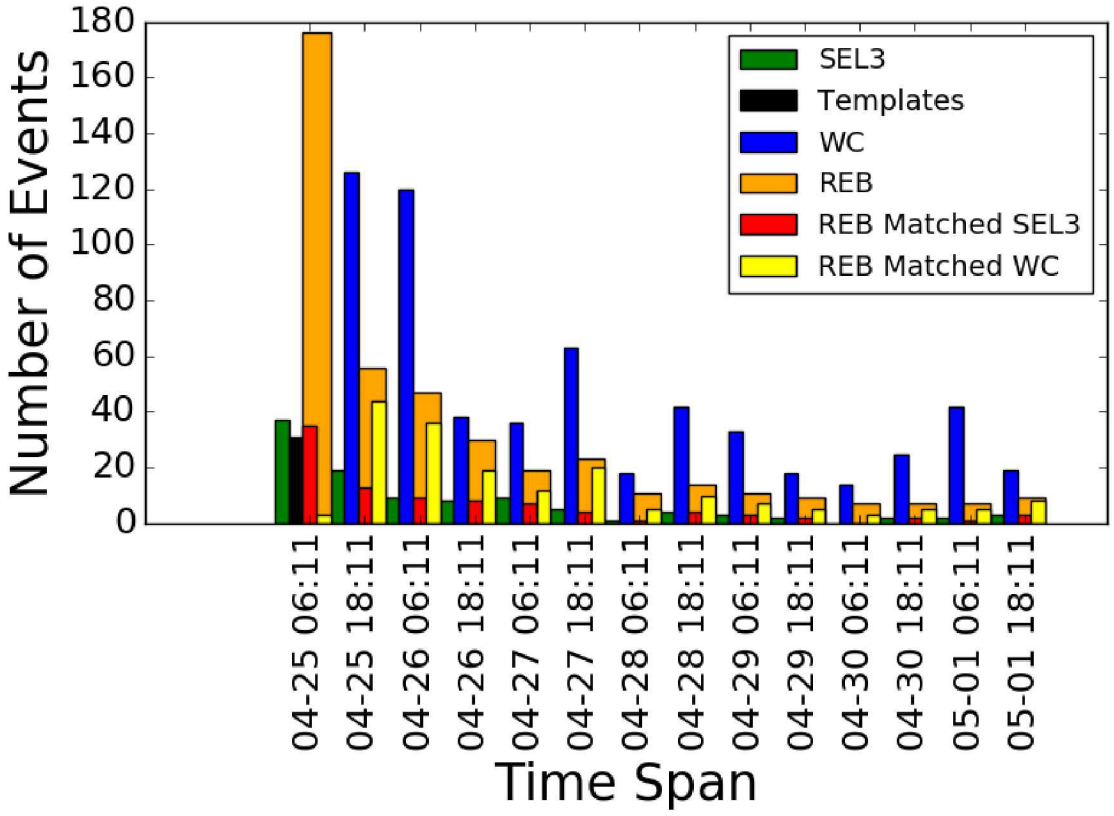

Figure 2-21. Comparison over 12-hour time increments of the number of 2015 Nepal aftershock the bulletins REB (orange), SEL3 (green), and WC (blue). The black bar indicates the number of template events. The events from the REB that matched SEL3 (red) and the events from the REB that matched the waveform correlation events (NDEF ≥ 1, yellow) are shown in the foreground of the REB (orange) bar.

Figure 2-21 shows that for the 2015 Nepal aftershock sequence, the IDC analysts had to build many events that were not in the automatic SEL3. In contrast, waveform correlation detected many of the manually built events. The analysis calculated the number of events found by waveform correlation that were not in the automatic SEL3 but were later added manually to the REB as an important measure of analyst effort during aftershock processing. Furthermore, the analysis calculated the number of events in the automatic SEL3 that were kept in the REB, indicating that the automatic pipeline detected correct events. Comparing the number of REB events detected by waveform correlation versus the REB events that were in the automatic SEL3 yields a ratio that estimates the workload reduction based on the number of REB events that are currently manually added by analysts but were detected by waveform correlation for the 2015 Nepal dataset. The estimated workload reduction for analyst-built events is shown by Equation 2-1, where the values for the variables are found in Table 2-8.

Equation 2-1: Estimated workload reduction for analyst-built events.

$$WR = \frac{A}{(B - C)} \times 100 = \frac{139}{(250 - 57)} = 72\%$$

Table 2-8. 2015 Nepal event counts used to calculate estimated workload reduction.

Variable	Description	# Events
	Number of waveform correlation (WC) events detected by 2 or more stations (NDEF ≥ 2)	182
	Number of all WC events (NDEF ≥ 1)	597
B	Number of REB events	250
C	Number of REB events matching SEL3	57
	Number of WC events (NDEF ≥ 1) matching REB	179
A	Number of REB events matching WC events (NDEF ≥ 1) not in SEL3	139
WR	**Estimated Workload Reduction**	**72%**

NOTE: Additional analysis is needed to provide alternate methods to calculate estimated analyst workload reduction.

The templates from the 2015 Nepal aftershock sequence produced many detections, as shown by the height of the WC bar for all 12-hour increments in Figure 2-21. The events found by waveform correlation that are not in the REB may be legitimate events but may be too small or may not be validated by multiple stations and do not meet the criteria for inclusion in the REB. Nonetheless, reviewing the result for the 2015 Nepal aftershock sequence motivates the adoption of waveform correlation for aftershock processing, particularly if the number of waveform correlation detections can be further refined to include criteria imposed on the REB events and thus reduce the number of waveform correlation events that must be discarded by analysts.

The numerator in Equation 2-1 has been plotted in Figure 2-22, where the number of events has been divided into groups by the number of detecting stations. The largest number of waveform correlation events are from single-station detections, but there are additional events detected by 3 to 10 stations that meet REB criteria.

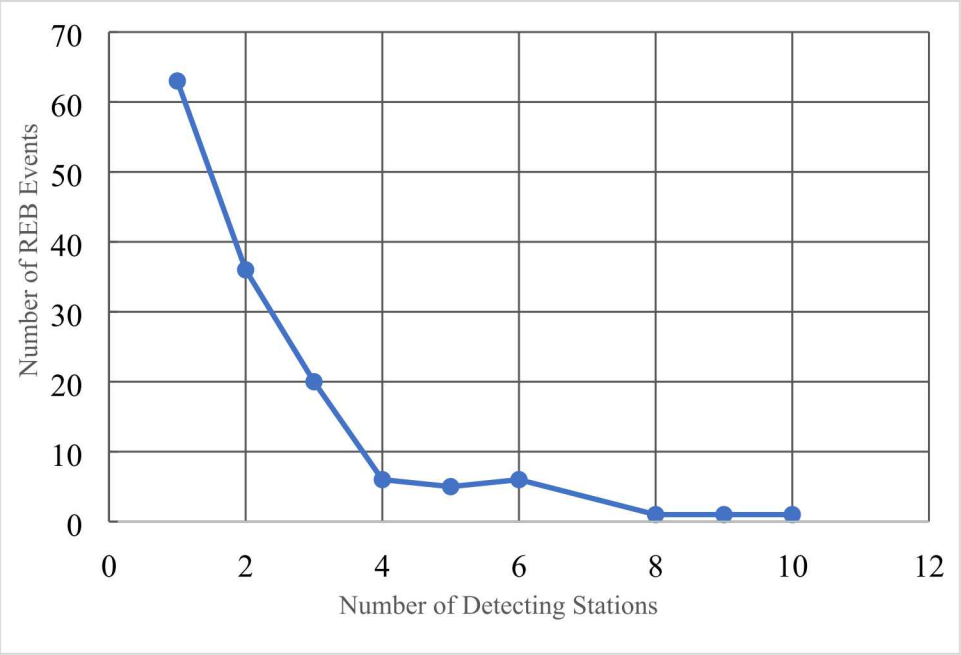

Figure 2-22. Number of 2015 Nepal REB events that were not in the automatic SEL3 but were detected by waveform correlation, plotted by the number of waveform correlation detecting stations/templates. Tolerances used are 1 degree for distance and ± 15 s for time.

2.5.4. 2015 Chile Events

The locations of events detected by waveform correlation for the 2015 Chile aftershock sequence are shown in the map (Figure 2-23). The size and color of the circle indicates the number of detecting templates, which usually corresponds to the number of detecting stations. There were 589 distinct events found by multistation validation with tolerances of 100 km and 15 s from waveform correlation jobs for the 12 IMS stations listed in Table 2-3; 175 of the events were detected by two or more stations and/or templates. A few events were located outside of the map extent and are not shown in this figure. This map includes single-template events, where a detection was made by one template but there were no other validating templates within the chosen tolerance. In the case of a single station event, the location is assumed to be the location of the template event.

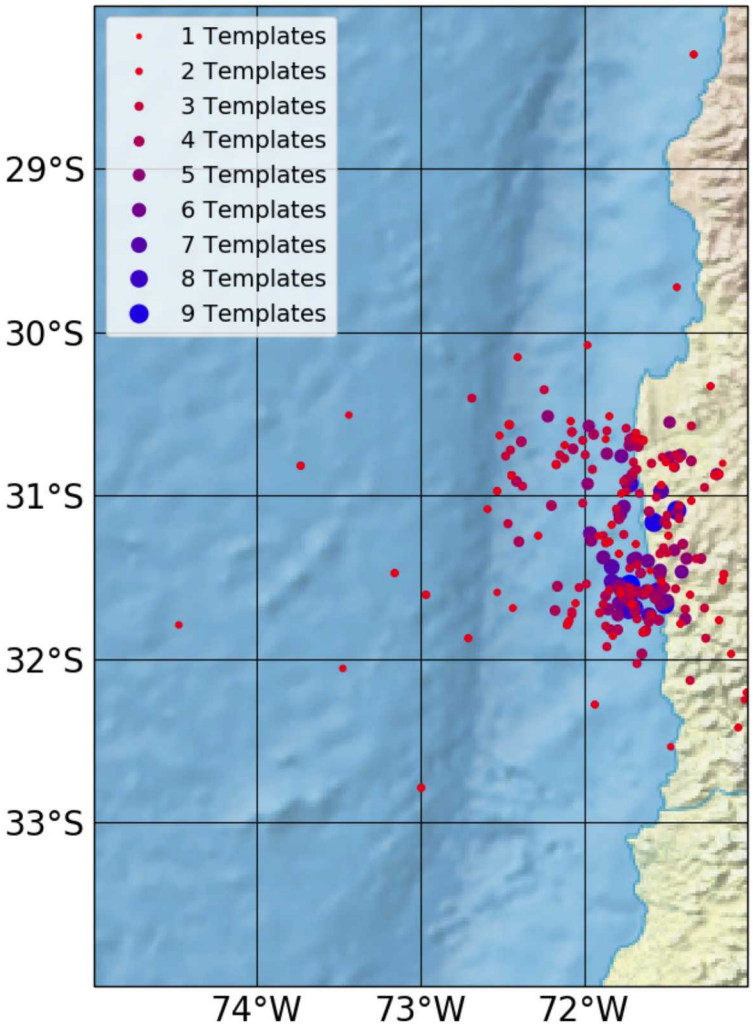

Figure 2-23. Map of the locations of the 589 2015 Chile aftershock events detected by waveform correlation. The size and color of the circle indicates the number of detecting templates.

An alternate way to visualize the events is shown by the bar charts in Figure 2-24. The bar chart shows count of events over 12-hour increments, spanning the entire week of the study of the 2015 Chile aftershock sequence. The first 12 hours includes the REB events (orange), SEL3 events (green) and the templates that were created from the SEL3 candidate events. Similar to the 2015 Nepal aftershock sequence, for 2015 Chile the IDC analysts had to add many events manually because the number of REB events far exceeds the number of SEL3 events. This fact is shown by directly comparing the number of REB events that match SEL3 (red), where the location and time must be within a radius of 1 degree and ±15 s to declare the origins the same. After the first 12 hours, the remaining 12-hour increments have two more additional bars that indicate the number of events detected by waveform correlation (blue) and the number of REB events that match waveform correlation events (yellow) within 1 degree and ±15 s.

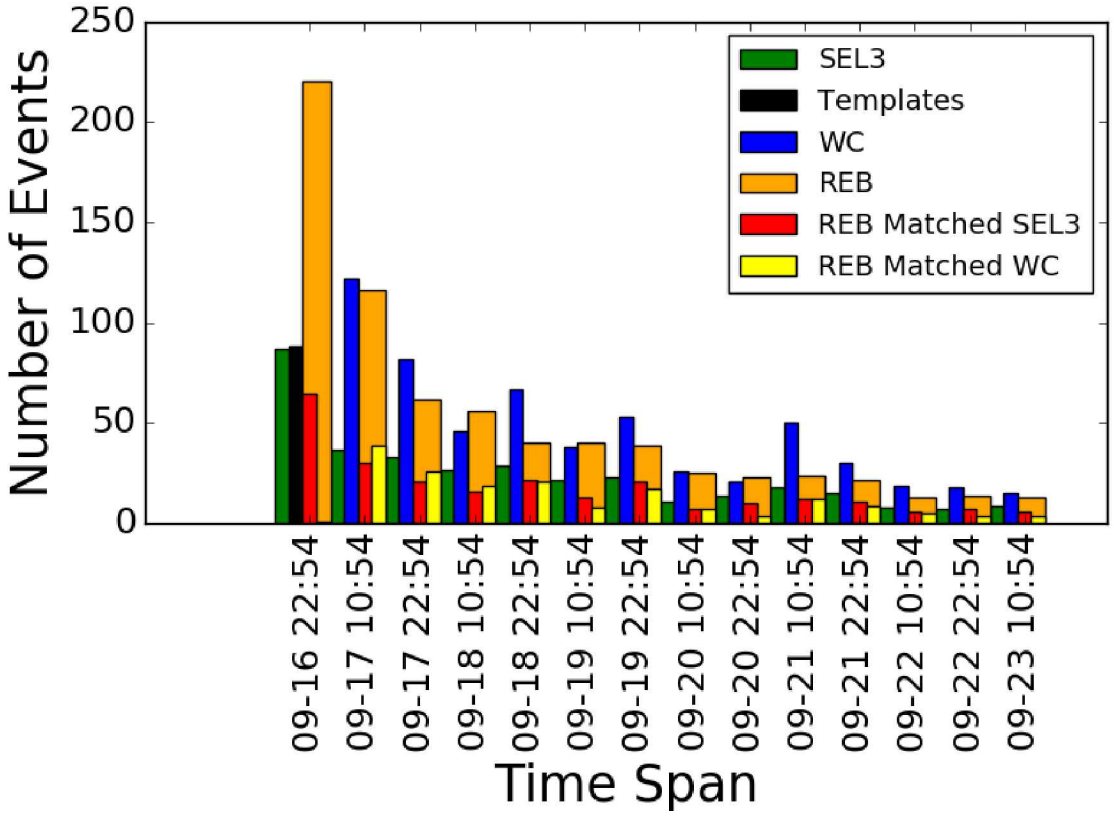

Figure 2-24. Comparison over 12-hour time increments of the number of 2015 Chile aftershock events in the REB (orange) and SEL3 (green), and waveform correlation templates (black) and events (blue). The events from the REB that matched SEL3 (red) and the events from the REB that matched the waveform correlation events (NDEF ≥ 1, yellow) are shown in the foreground of the REB (orange) bar.

Figure 2-24 shows that waveform correlation detected many of the manually built events. Similarly, to the 2015 Nepal aftershock sequence, the estimated workload reduction for analyst-built events was calculated by Equation 2-1, where the values for the variables are found in Table 2-9.

Table 2-9. 2015 Chile event counts used to calculate estimated workload reduction.

Variable	Description	# Events
	Number of Waveform correlation (WC) events detected by 2 or more stations (NDEF ≥ 2)	175
	Number of all WC events (NDEF ≥ 1)	589
B	Number of REB events	487
C	Number of REB events matching SEL3	182
	Number of WC events (NDEF ≥ 1) matching REB	175
A	Number of REB events matching WC events (NDEF ≥ 1) not in SEL3	68
WR	**Estimated Workload Reduction**	**22%**

The numerator of Equation 2-1 has been plotted in Figure 2-25, where the number of events has been divided into groups by the number of detecting stations. The largest number of waveform correlation events are from single-station detections, but there are additional events that meet REB criteria with 3 to 9 detecting stations.

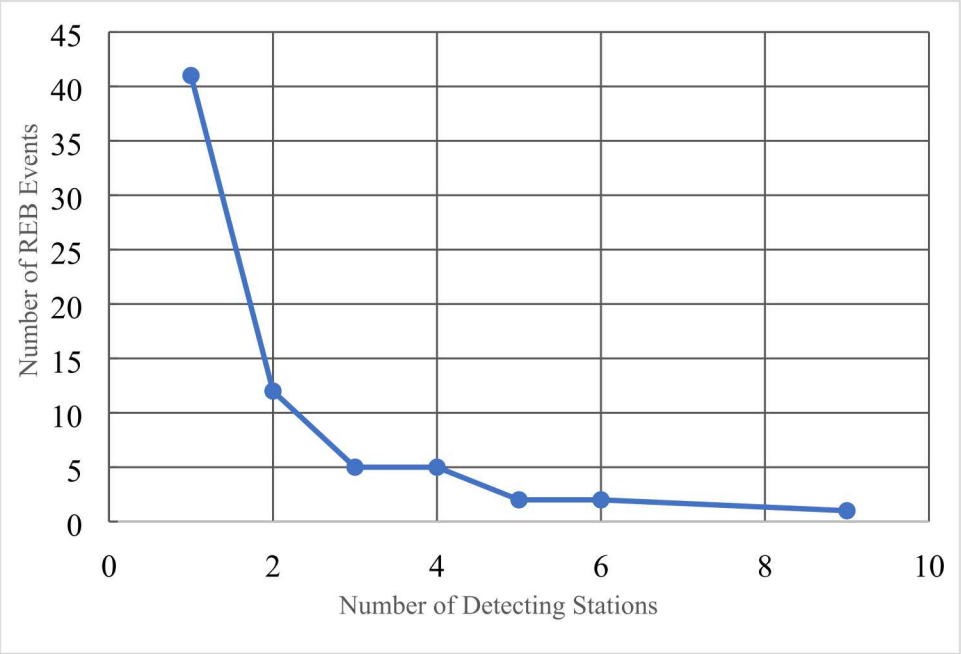

Figure 2-25. Number of 2015 Chile REB events that were not in the automatic SEL3 but were detected by waveform correlation, plotted by the number of waveform correlation detecting stations/templates. The comparison tolerances for event origins were a radial distance of 1 degree and time of ± 15 s.

2.5.5. 2011 Tohoku Events

The locations of events detected by waveform correlation for the 2011 Tohoku aftershock sequence are shown in a series of maps (Figure 2-26 to Figure 2-32); the legend on the first figure applies to every figure in the series. The size and color of the unfilled circle indicates the number of detecting templates, which usually corresponds to the number of detecting stations. However, in some cases an event can be detected by two templates from the same station, such as the case where there are two phase templates for the same event (i.e., Pn and P), and this explains how we can have as many as 17 detecting templates for a multistation validation job with only 12 stations. The 2011 Tohoku sequence covered a larger geographical area than the prior two sequences, and an abbreviated parameterization study of tolerances (similar to that described in 2.5.2) led us to choose more relaxed tolerances for this aftershock sequence. There were 11033 distinct origins found by multistation validation with tolerances of 150 km and 30 s from waveform correlation jobs for the 12 IMS stations listed in Table 2-5; 4840 of the events were detected by two or more stations. These maps show only events detected by 3 or more stations.

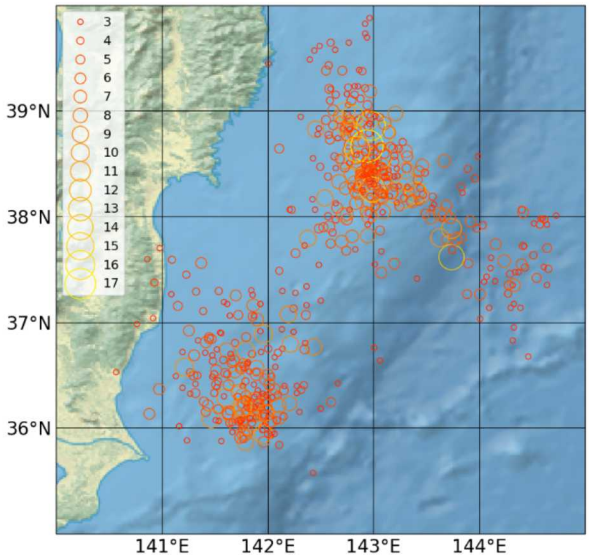

Figure 2-26. 2011 Tohoku 567 aftershock events detected by 3 or more stations during the first 12-24 hours after the mainshock. The size and color of the circle indicates the number of detecting templates.

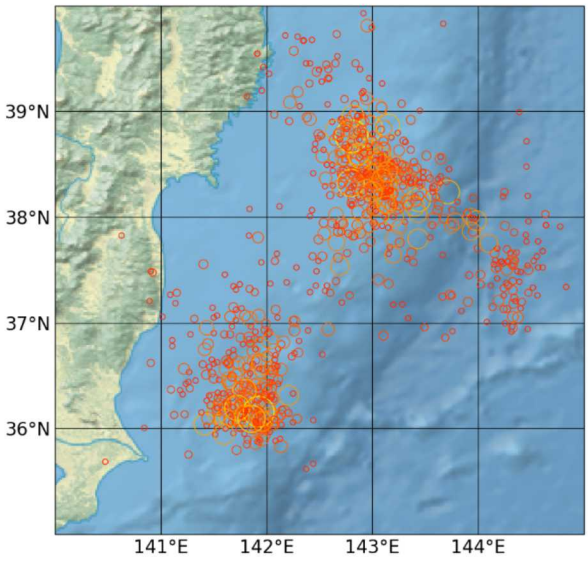

Figure 2-27. 853 events detected on day 2.

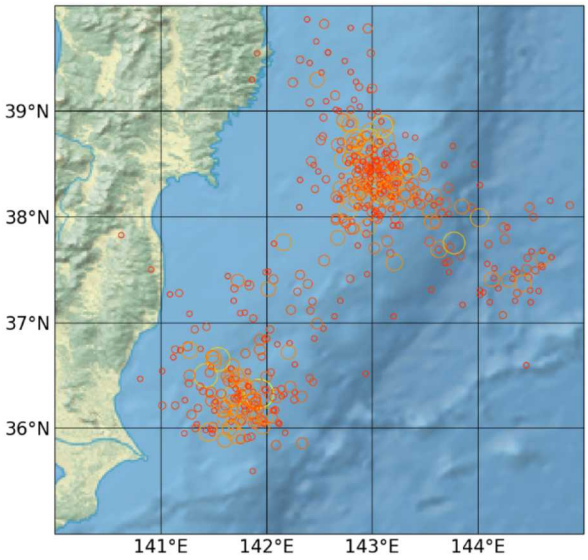

Figure 2-28. 511 events detected on day 3.

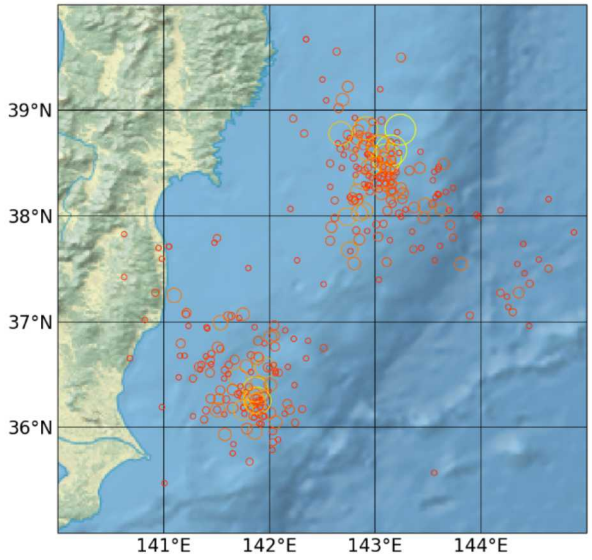

Figure 2-29. 326 events detected on day 4.

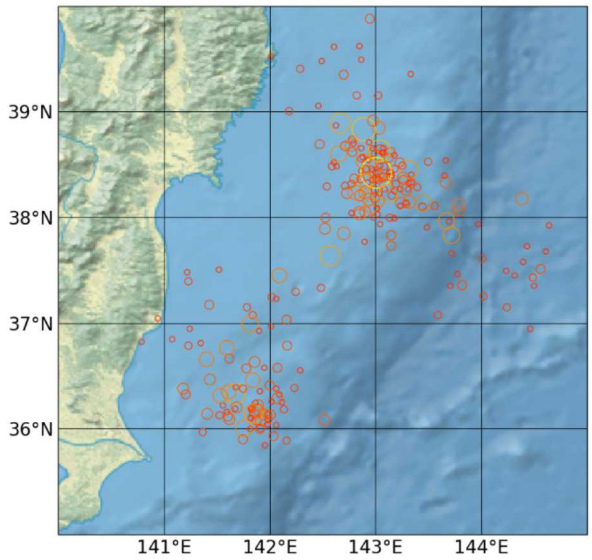

Figure 2-30. 245 events detected on day 5.

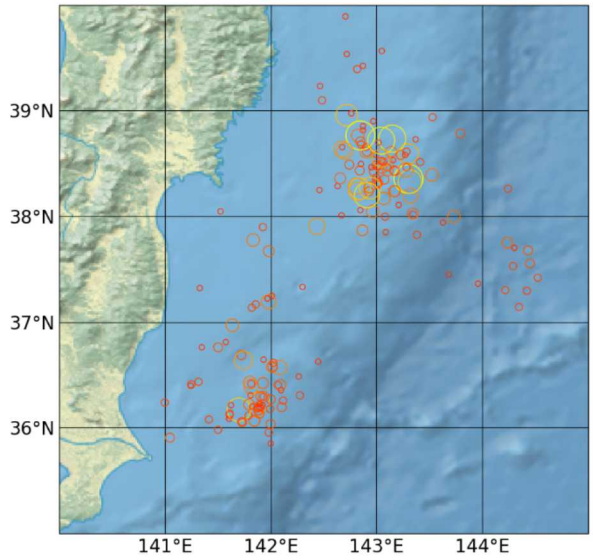

Figure 2-31. 172 events detected on day 6.

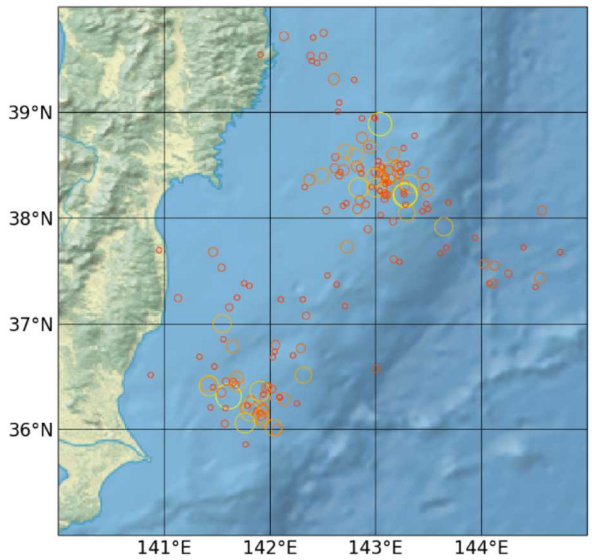

Figure 2-32. 175 events detected on day 7.

An alternate way to visualize the events detected by 3 or more stations is shown by the bar charts in Figure 2-33, which shows count of events over 12-hour increments, spanning the entire week of the study of the 2011 Tohoku aftershock sequence. The first 12 hours includes the REB events (orange), SEL3 events (green) and the templates that were created from the SEL3 candidate events. Similar to the 2015 Nepal aftershock sequence, for 2011 Tohoku the IDC analysts added many events manually because the number of REB events far exceeds the number of SEL3 events. This

fact is shown by directly comparing the number of REB events that match SEL3 (red), where the location and time must be within a radius of 1 degree and ±15 s to declare the origins the same. After the first 12 hours, the remaining 12-hour increments have two more additional bars that indicate the number of events detected by waveform correlation (blue) and the number of REB events that match waveform correlation events (yellow) within 1 degree and ±15 s.

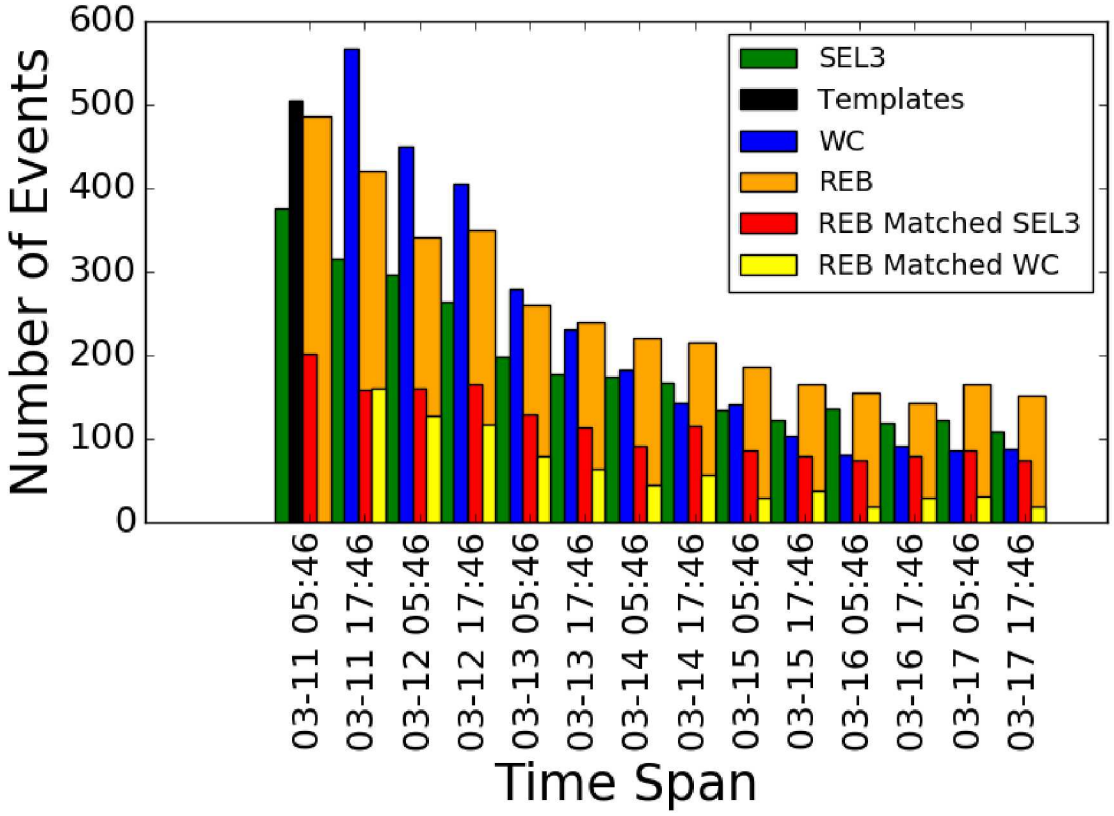

Figure 2-33. Comparison over 12-hour time increments of the number of 2011 Tohoku aftershock events in the REB (orange) and SEL3 (green), and waveform correlation templates (black) and events (NDEF ≥ 3, blue). The events from the REB that matched SEL3 (red) and the events from the REB that matched the waveform correlation events (NDEF ≥ 3, yellow) are shown in the foreground of the REB (orange) bar.

Figure 2-33 shows that waveform correlation detected many of the manually built events with 3 or more detecting templates. Similar to the 2015 Nepal aftershock sequence, the estimated workload reduction for analyst-built events was calculated by Equation 2-1, where the values for the variables are found in Table 2-10. The waveform correlation events included in the estimate of workload reduction for the 2011 Tohoku aftershock sequence had at least 2 detecting templates and/or stations.

Table 2-10. 2011 Tohoku event counts used to calculate estimated workload reduction.

Variable	Description	# Events
	Number of waveform correlation (WC) events detected by 2 or more stations (NDEF ≥ 2)	4840
	Number of all WC events (NDEF ≥ 1)	11033
B	Number of REB events	3015
C	Number of REB events matching SEL3	1415
	Number of WC events (NDEF ≥ 2) matching REB	1494
A	Number of REB events matching WC events (NDEF ≥ 2) not in SEL3	624
WR	**Estimated Workload Reduction**	**39%**

The numerator of Equation 2-1 has been plotted in Figure 2-34, where the number of events has been divided into groups by the number of detecting stations. The largest number of waveform correlation events are from single-station detections, but there are additional events that meet REB criteria with 3 to 9 detecting stations.

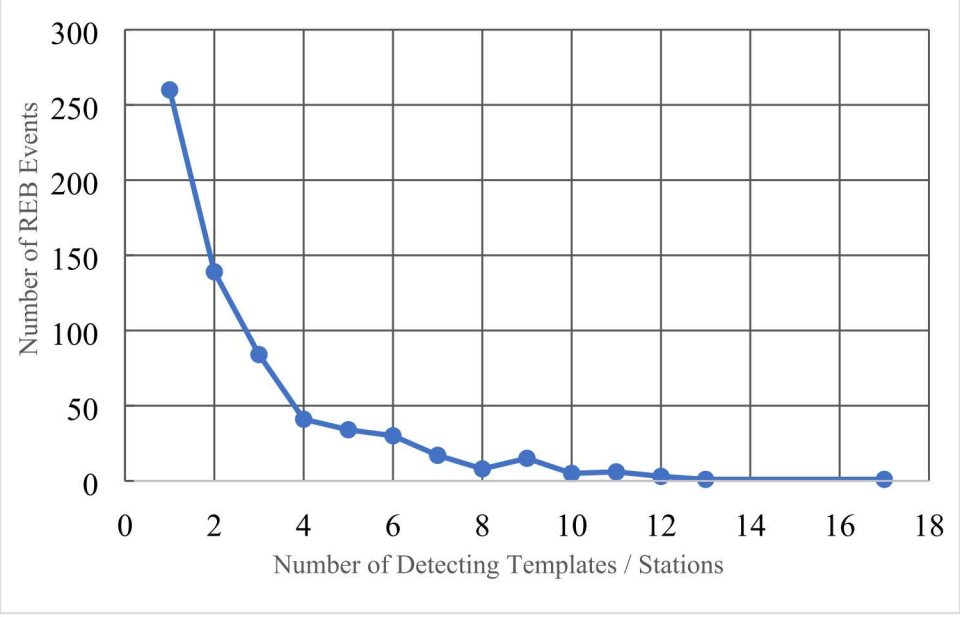

Figure 2-34. Number of 2011 Tohoku REB events that were not in the automatic SEL3 but were detected by waveform correlation events, plotted by the number of waveform correlation detecting stations/templates. The comparison tolerances for event origins were a radial distance of 1 degree and time of ± 15 s.

3. DISCUSSION

The focus of this research study was to apply waveform correlation to aftershock sequences deemed particularly problematic for the IDC to find out if the technique could reduce analyst workload to produce the REB. Three of the four aftershock sequences identified by the IDC were studied using SNL's SeisCorr application for waveform correlation; the remaining sequence, 2018 Papua New Guinea, was excluded due to funding limitations. In all cases, SeisCorr detected candidate events that matched REB events within a tolerance of 1 degree and ±15 s, but that have no corresponding match in the SEL3 bulletin. Thus, we conclude that waveform correlation has the potential to reduce analyst workload for aftershock sequences but recommend additional research to quantify the workload reduction accurately.

3.1. Experimental Setup

The experimental setup described in the project launch meeting emphasized that operational constraints must be adhered to when creating template waveforms. Previous studies of aftershock sequences often use waveforms from all aftershock events to detect new aftershock events because the studies are done on historical data. Those studies showed impressive results but did not address the operational realities of choosing templates as the aftershock sequence evolves. This study offers insight into the choices available to an operational monitoring agency. The choices that were allowed for template waveforms included:

1. events from SEL3, available within 12 hours after the mainshock, or
2. historical events from the REB that were three or more days prior to the mainshock.

For the SeisCorr research study, we chose to use SEL3 events for the waveform templates because we had not tried this approach in the past and wanted to determine if it was feasible to use templates from the automatic SEL3. Moreover, historical events from the REB may be located more accurately but offer the complication that the source mechanism may be different and could result in detections that were geographically located within a region of aftershock events but were not aftershock events.

Further research that compares detections from historical events versus automatically built events may provide insight into whether options 1 or 2 are the better bulletin for waveform templates for aftershock events.

3.2. Waveform Templates

In an aftershock sequence, events occur in close proximity in both space and time, making the selection of templates and template windows more challenging than for a typical waveform correlation study of seismic events that are sparse in location and time. SeisCorr automatically uses arrivals from bulletin events to window waveform templates according to user-defined parameters such as total template duration in seconds and the number of seconds preceding the arrival; for this study, the values of 15 seconds were chosen for the template duration, with 2 seconds preceding the arrival. Typically, a user-defined STA/LTA threshold is applied to guarantee that a signal is present within the window. Moreover, such user-defined parameters may be chosen per template library, so template durations may vary by station and/or phase.

There are several types of problems that are encountered with SeisCorr templates. Although the templates are screened to pass an STA/LTA threshold, it is possible that an unrelated signal may

overlap within the template window, thus meeting the threshold criteria but not accurately detecting the expected signal when correlated with continuous data. The templates for the aftershock study were not reviewed and pruned manually, and examples of overlapping signals have been observed in the template libraries. However, given the short timeframe of this study, it is likely that most of the overlapping signals are also aftershock events that occur later during the sequence. For such templates, we expect the detections to be valid, but these detections may not be associated with the correct candidate events. An operational pipeline may require algorithms to screen templates for overlapping signals, especially overlapping aftershock events. For arrays, it may be possible to develop an algorithm that includes only templates that demonstrate a moveout across elements that matches the mainshock moveout, thus enforcing a location-specific template filter. More research on the selection of waveform templates for aftershock studies is needed.

This study created template libraries from approximately a dozen IMS stations for each aftershock sequence; the number of stations was limited because the process of creating template libraries and running correlation jobs with the libraries are interactive features in SeisCorr. In an automated pipeline, it would make sense to include all the stations of the primary IMS network in the process; thus, with more template libraries and more detecting stations, it seems reasonable to expect that the results of waveform correlation using IMS network would exceed the results reported in this study.

3.3. Template Thresholds

SeisCorr sets individual template thresholds based on background noise characteristics using the time-reverse method. The template thresholds set for this aftershock study exhibited statistical parameters that varied widely by station. For the convenience of the reader, Table 3-1 juxtaposes the threshold figures for the three aftershock sequences to illustrate the point that some stations have far less variability in median template threshold values than others; Tohoku especially exhibits this behavior for some stations.

We performed analysis to determine if a pattern exists that would be possible to exploit for setting template thresholds for aftershock sequences in the future. The original figures shown in row a) ordered the stations alphabetically, and no pattern in median thresholds was obvious across the collection of stations. Row b) orders the stations by distance from the mainshock, and a general rising trend of median threshold value versus distance appears but with outliers such as KSRS for 2015 Nepal and NOA and AKASG for 2011 Tohoku. Row c) orders the stations by number of channels, and within a group of stations that have the same number of channels, the stations are ordered by distance; including the number of channels brings the outliers KSRS, NOA, and AKASG into the prevailing trend.

We postulate that the median threshold value may be influenced by a function that is based upon the number of recording channels and the distance from the earthquake, yet that function is more complex than the simple ordering demonstrated by row c) in the table. For example, consider that for the 2015 Nepal aftershock sequence, array CMAR has the closest epicentral distance; we observe that the median threshold value is higher than some stations with more channels, yet lower than other stations with more channels. A similar example can be seen in the 2011 Tohoku aftershock sequence with the array USRK. Most of the stations for the 2015 Chile aftershock sequence were three-component stations, so the trend that arises for this sequence is almost exclusively influenced by distance. Further research is needed to explore whether finding a function that predicts median template threshold values will aid monitoring agencies in developing template libraries for aftershock sequences.

Table 3-1. Template thresholds by aftershock sequence. a) Stations are ordered alphabetically. b) Stations are ordered by increasing epicentral distance to the mainshock. c) Stations are ordered first by increasing number of channels, then by increasing epicentral distance to the mainshock.

	Nepal	Chile	Tohoku
a	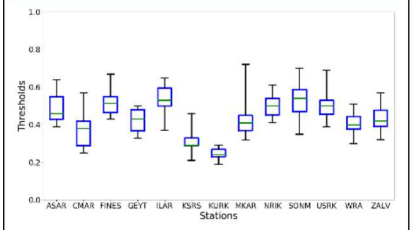	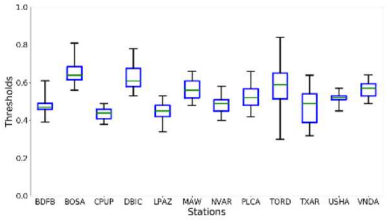	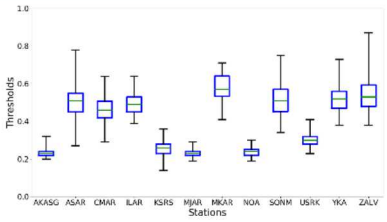
	Figure 2-5	Figure 2-9	Figure 2-13
b	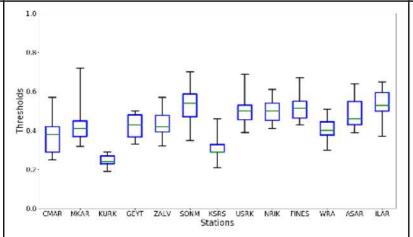	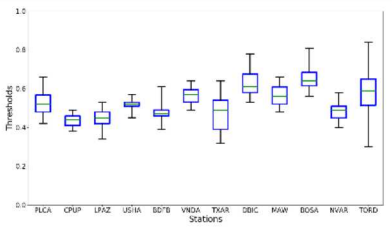	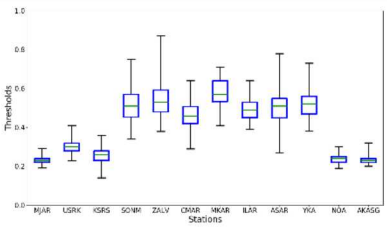
c	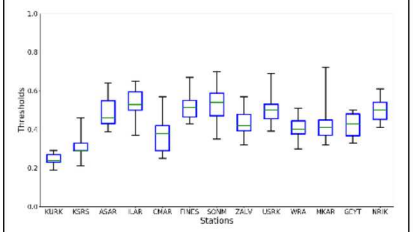	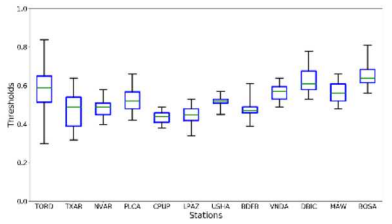	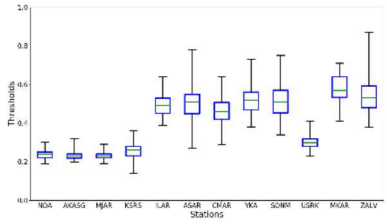

3.4. Candidate Events

SeisCorr includes the multistation validation feature to group detections into candidate events. A candidate event with detections by multiple stations is generally considered more reliable than a detection by a single station. For the aftershock study, we have chosen to include results from candidate events based on any number of detecting stations, including only one station. We included single-station events because multistation validation is a method of grouping detections that is less sophisticated than the associators employed by operational pipelines. We did not want to exclude detections from single stations that may be grouped with other detections using an associator (e.g., NET-VISA [9]), even though they were unassociated after multistation validation.

3.5. Summary

The metric chosen to report estimated analyst workload reduction compares the number of REB events that were detected by waveform correlation but were not in the SEL3 within a time and location tolerance. This metric was chosen because analysts must find and build these events manually, and waveform correlation shows that it can assist by reducing the number of events built this way.

However, the chosen workload reduction metric is dependent upon the number of REB events that the analysts accepted from SEL3, showing only the incremental improvement that waveform correlation can potentially make to the existing pipeline. We offer here an alternate metric, the effectiveness of waveform correlation for detecting aftershock events, which is independent of SEL3. As indicated in Equation 3-1, effectiveness is the proportion of events from the REB that are detected by waveform correlation. This alternate metric assesses the potential effectiveness of waveform correlation in the IDC pipeline at finding REB events. As reported in Table 3-2, the effectiveness for 2011 Tohoku and 2015 Chile is 50% and 36% respectively, versus the workload reduction values of 39% and 22%.

Equation 3-1: Alternate estimation of effectiveness of waveform correlation.

$$Effectiveness = \frac{REB\ events\ matching\ WC}{REB\ events} \times 100$$

Table 3-2. Alternate estimation of effectiveness of waveform correlation.

Description	Nepal 2015	Chile 2015	Tohoku 2011
REB Events	250	487	3015
REB Events matching waveform correlation events within 1 degree, ± 15 s	179	175	1494
Effectiveness	72%	36%	50%

We offer the alternate calculation of effectiveness to encourage the development of other metrics for workload reduction. For example, waveform correlation is known for detecting events that are an order of magnitude smaller than the template waveform. Waveform correlation will not reduce the overall workload of the analyst if more time must be spent rejecting small events. The approach of including waveform correlation detections as input to the associator, currently under investigation by the IDC, may prevent flooding the analyst with small events.

The conclusion of this report is that waveform correlation shows promise as a technique for reducing human analyst workload during a large aftershock sequence. The addition of valid waveform correlation events to SEL3 shows that fewer events would have to be manually built by the analysts if WC were incorporated into the pipeline. We recommend that further research focuses on the automatic selection of the correlation detections that are useful to the analysts, while ignoring correlation detections of aftershocks that are below pragmatic detection thresholds.

REFERENCES

[1] Slinkard, M., S. Heck, D. Schaff, N. Bonal, D. Daily, C. Young, and P. Richards (2016). Detection of the Wenchuan Aftershock Sequence Using Waveform Correlation with a Composite Regional Network, *Bull. Seismol. Soc. Am.* **106**, 1371-1379. doi: 10.1785/0120150333.

[2] Slinkard, M. E., D. B. Carr, and C. J. Young (2013). Applying waveform correlation to three aftershock sequences, *Bull. Seismol. Soc. Am.* **103**, 675-693. doi: 10.1785/0120120058.

[3] Slinkard, M., D. Schaff, N. Mikhailova, S. Heck, C. Young, and P. G. Richards (2014). Multistation validation of waveform correlation techniques as applied to broad regional monitoring, *Bull. Seismol. Soc. Am.* **104**, 2768-2781. doi: 10.1785/0120140140.

[4] Anderson, J., W. E. Farrell, K. Garcia, J. Given, H. Swanger (1990). Center for Seismic Studies Version 3 Database: Schema Reference Manual. *Technical Report C90-01*. http://jkmacc-lanl.github.io/pisces/data/Anderson1990.pdf

[5] Ganter, T., A. Sundermier, and S. Ballard (2018). Alternate Null Hypothesis Correlation: A New Approach to Automatic Seismic Event Detection, *Bull. Seismol. Soc. Am.* **108**, 3528-3547. doi: 10.1785/0120180074.

[6] Di Giacomo, D., D. A. Storchak, N. Safronova, P. Ozgo, J. Harris, R. Verney, and I. Bondár (2014). A New ISC Service: The Bibliography of Seismic Events, *Seismol. Res. Lett.*, **85**, 2, 354-360, doi: 10.1785/0220130143.

[7] International Seismological Centre, On-line Event Bibliography, http://www.isc.ac.ud/event_bibliography, Internatl. Seis. Cent., Thatcham, United Kingdom, 2015, https://doi.org/10.31905/EJ3B5LV6.

[8] Harris, D. B., and T. Kvaerna (2010). Superresolution with seismic arrays using empirical matched field processing, *Geophys. J. Int.* **182**, no. 3, 1455-1477. doi: 10.1111/j.1365-246x.2010.04684.x.

[9] Arora, N. S., S.Russel, and E. Sudderth (2013). NET-VISA: Network processing vertically integrated seismic analysis, *Bull. Seismol. Soc. Am.*, **103**, no. 2A, 709-729. doi: 10.1785/0120120107.

DISTRIBUTION

Email—Internal

Name	Org.	Sandia Email Address
Technical Library	01177	libref@sandia.gov

This page left blank

This page left blank

Sandia National Laboratories

Sandia National Laboratories is a multimission laboratory managed and operated by National Technology & Engineering Solutions of Sandia LLC, a wholly owned subsidiary of Honeywell International Inc. for the U.S. Department of Energy's National Nuclear Security Administration under contract DE-NA0003525.